

JET PROPULSION LABORATORY

SIRTF IPF REPORT

JPL ID203118

November 20, 2003

**SIRTF INSTRUMENT POINTING FRAME
KALMAN FILTER EXECUTION SUMMARY**

IPF RUN NUMBER: 203118

REPORT TYPE: IOC EXECUTION (COARSE)

PRIME FRAME: MIPS_70um_fine_center (118)

INFERRRED FRAMES: (119) (120) (124) (127) (117)

IPF TEAM

Autonomy and Control Section (345)

Jet Propulsion Laboratory

California Institute of Technology

4800 Oak Grove Drive

Pasadena, CA 91109

Contents

1 IPF EXECUTION SUMMARY	5
2 IPF INPUT FILE HISTORY	9
3 IPF EXECUTION RESULTS	12
3.1 IPF EXECUTION OUTPUT PLOTS	12
3.2 IPF OUTPUT DATA (IF MINI FILE)	38
3.3 IPF EXECUTION LOG	42
4 COMMENTS	45

List of Figures

1.1 A-priori and a-posteriori IPF frames	5
1.2 A-priori and a-posteriori IPF frames (ZOOMED)	8
2.1 Scenario Plot	9
2.2 Attitude file edit history	10
2.3 Centroid file edit history	10
2.4 Oriented Pixel Coords of Centroid Meas. Edited Centroids	11
3.1 TPF coords of measurements and a-priori predicts	14
3.2 Oriented Pixel Coords of measurements and a-priori predicts	14
3.3 Oriented (W,V) Pixel Coords of A-Priori Prediction Error Quiver Plot	15
3.4 A-priori prediction error (Science Centroids)	15
3.5 Oriented Pixel Coords of measurements and a-priori predicts (PCRS only)	16
3.6 Oriented Pixel Coords of measurements and a-priori predicts (Zoomed, PCRS only)	16
3.7 Oriented (W,V) Pixel Coords of A-Priori PCRS Prediction Error Quiver Plot	17
3.8 A-priori PCRS prediction error	17
3.9 IPF execution convergence, chart 1	18
3.10 IPF execution convergence, chart 2	18
3.11 Parameter uncertainty convergence	19
3.12 IPF parameter symbol table	19
3.13 KF parameter error sigma plots	20
3.14 LS parameter error sigma plot	20

3.15 KF and LS parameter error sigma plot	21
3.16 Oriented Pixel Coords of meas. and a-posteriori predicts	22
3.17 Oriented Pixel Coords of meas. and a-posteriori predicts (attitude corrected)	22
3.18 KF innovations with (o) and w/o (+) attitude corrections	23
3.19 Histograms of science a-posteriori residuals (or innovations)	23
3.20 A-Posteriori Science Centroid Prediction Error Quiver (Att. Cor.)	24
3.21 Normalized A-Posteriori Science Centroid Prediction Errors	24
3.22 KF innovations with (o) and w/o (+) attitude corrections (PCRS)	25
3.23 Histograms of PCRS a-posteriori residuals (or innovations)	25
3.24 A-posteriori PCRS Prediction Summary	26
3.25 A-posteriori PCRS Prediction (PCRS 1 Only)	27
3.26 A-posteriori PCRS Prediction (PCRS 2 Only)	27
3.27 A-Posteriori PCRS Prediction Errors Quiver (Att. Cor.)	28
3.28 Normalized A-Posteriori PCRS Prediction Errors	28
3.29 W-axis KF innovations and 1-sigma bound	29
3.30 V-axis KF innovations and 1-sigma bound	29
3.31 Array plot with (solid) and w/o (dashed) optical distortion corrections	30
3.32 Optical Distortion Plot: total (x5 magnification)	30
3.33 Optical Distortion Plot: constant plate scales (x5 magnification)	31
3.34 Optical Distortion Plot: linear plate scale (x5 magnification)	31
3.35 Optical Distortion Plot: gamma terms (x5 magnification)	32
3.36 Scan Mirror Chops	32
3.37 IPF Frame Reconstruction	33
3.38 Center Pixel Reconstruction	33
3.39 Estimated attitude corrections (Body frame)	34
3.40 Estimated attitude error sigma plot (Body frame)	34
3.41 Thermo-mechanical boresight drift (equiv. angle in (W,V) coords)	35
3.42 Thermo-mechanical boresight drift (equiv. angle in Body frame)	35
3.43 Gyro drift bias contribution (equiv. rate in (W,V) coords)	36
3.44 Gyro drift bias contribution (equiv. angle in (W,V) coords)	36
3.45 Gyro drift bias contribution (equiv. angle in Body frame)	37

List of Tables

1.1	IPF filter input files	6
1.2	IPF filter execution configuration	6
1.3	IPF filter execution mask vector assignment	6
1.4	IPF calibration error summary ([arcsec], 1-sigma, radial)	7
1.5	Science measurement prediction error summary (1-sigma)	7
1.6	IPF Brown angle summary	8
2.1	IPF input file begin and end times	9
2.2	IPF input file editing status	9
2.3	List of Removed Centroids (Original CA File Row Index)	11
2.4	List of Removed PCRS Centroids (Original CB File Row Index)	11
3.1	Table of figures I (IPF run)	12
3.2	Table of figures II (IPF run)	13
3.3	PCRS measurement prediction error summary	26

1 IPF EXECUTION SUMMARY

This report summarizes the SIRTF Instrument Pointing Frame (IPF) Kalman Filter execution associated with run file: RN203118. In particular, this Focal Point Survey calibrates the instrument: MIPS_70um_fine_center (118), as part of the IOC Coarse Survey. The main calibration results from the IPF filter execution have been documented in IF203118 typically stored in the mission archive DOM collection IPF_IF. This report only summarizes the main aspects of the run, and does not substitute for the full information contained in the IF file.

Section 1 summarizes the filter execution results. The filter configurations are tabulated in Table 1.2 and the mask vector assignments are tabulated in Table 1.3. A total of 17 state parameters are estimated in this run. The overall End-to-End pointing performances are tabulated in Table 1.4. The prediction residuals throughout the estimation processes are tabulated in Table 1.5. Section 3 summarizes resulting plots, a mini summary of the IF IPF output file, and the execution log. Section 4 captures the user comments that are specific to this particular run.

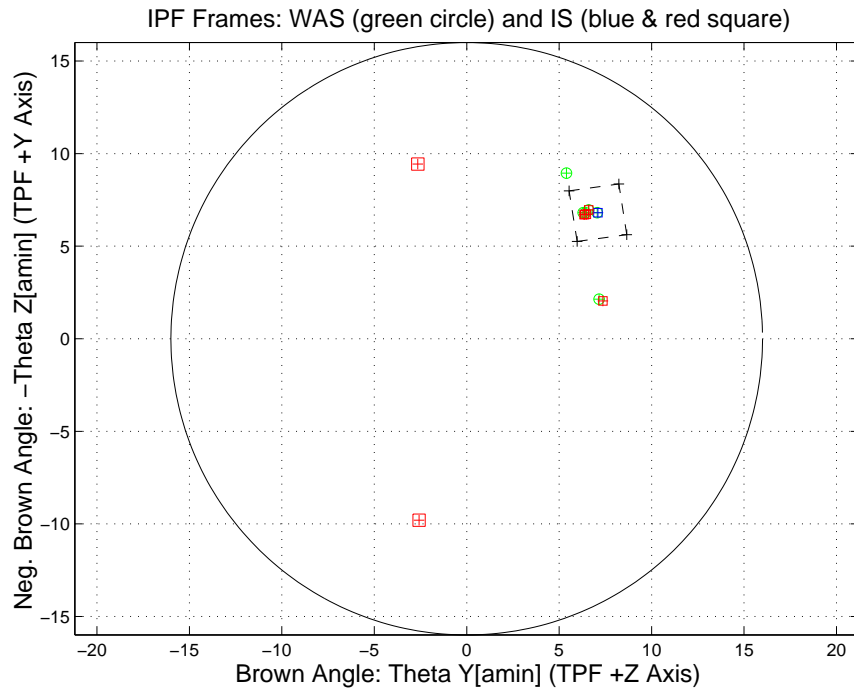


Figure 1.1: A-priori and a-posteriori IPF frames

RAW	FINAL (After Editing)
AA101118	AA101118
AS101118	AS101118
CA201118	CA201118
CB102118	CB103118
CS201118	CS201118

Table 1.1: IPF filter input files

EXECUTION CONFIGURATION ITEM	CURRENT STATUS
IPF Filter Version Used	IPF.V3.0.0B
Frame Table Version Used	BodyFrames_FTU_13Aa
Scan-Mirror Employed?	YES
IPF Filter Mode	NORMAL-MODE(0)
SLIT-MODE Operation	DISABLED
Kalman Filter Operation	ENABLED
Least-Squares Data Analysis	ENABLED
IBAD Screening	ENABLED
User-Specified Data Editing	DISABLED
Total Number of Iterations	30
LS Residual Sigma Scale	6.44649530E-001
Total Number of Maneuvers	10

Table 1.2: IPF filter execution configuration

Con. Plate Scale			Γ Dependent				Γ^2 Dependent				Linear Plate Scale						Mirror			
a_{00}	b_{00}	c_{00}	a_{10}	b_{10}	c_{10}	d_{10}	a_{20}	b_{20}	c_{20}	d_{20}	a_{01}	b_{01}	c_{01}	d_{01}	e_{01}	f_{01}	α	β		
1	2	3	4	5	6	7	8	9	10	11	12	13	14	15	16	17	18	19		
1	1	1	0	0	0	0	0	0	0	0	0	0	0	0	0	0	1	1		
IPF (T)			Alignment R						Gyro Drift Bias											
θ_1	θ_2	θ_3	a_{rx}	a_{ry}	a_{rz}	b_{rx}	b_{ry}	b_{rz}	c_{rx}	c_{ry}	c_{rz}	b_{gx}	b_{gy}	b_{gz}	c_{gx}	c_{gy}	c_{gz}			
20	21	22	23	24	25	26	27	28	29	30	31	32	33	34	35	36	37			
1	1	1	1	1	1	0	0	0	0	0	0	1	1	1	1	1	1			

Table 1.3: IPF filter execution mask vector assignment

FOCAL PLANE SURVEY ANALYSIS: IOC Coarse Survey.

INSTRUMENT NAME: MIPS_70um_fine_center NF: 118

PIX2RADW: 2.47365083E-005 [rad/pixel] = 5.1023E+000 [arcsec/pixel]

PIX2RADV: 2.54648081E-005 [rad/pixel] = 5.2525E+000 [arcsec/pixel]

FRAME	DESCRIPTION	IPF ¹	SF ²	TOTAL	REQ
118(P)	MIPS_70um_fine_center	0.2889	0.0855	0.3013	1.12
119(I)	MIPS_70um_fine_FOV1	0.1788	0.0855	0.1982	N/A
120(I)	MIPS_70um_fine_FOV2	0.9994	0.0855	1.0031	N/A
124(I)	MIPS_70um_fine_FOV3	0.1620	0.0855	0.1832	N/A
127(I)	MIPS_70um_fine_FOV4	0.2169	0.0855	0.2332	N/A
117(I)	MIPS_SED_8	0.2027	0.0855	0.2200	N/A

Table 1.4: IPF calibration error summary ([arcsec], 1-sigma, radial)

RMS METRIC	A PRIORI ³	A POSTERIORI ³	ATT. CORRECTED ⁴	UNITS
Radial	4.7159	3.0025	2.9908	arcsec
W-Axis	3.9118	2.5033	2.4883	arcsec
V-Axis	2.6338	1.6579	1.6592	arcsec
Radial	0.9161	0.5834	0.5811	pixels
W-Axis	0.7667	0.4906	0.4877	pixels
V-Axis	0.5014	0.3156	0.3159	pixels

Table 1.5: Science measurement prediction error summary (1-sigma)

¹IPF filter removes systematic pointing errors due to: thermomechanical alignment drift (Body to TPF), gyro bias and bias drift, centroiding error, attitude error, and optical distortion. IPF SIGMA presented here is “Scaled” by the Least Squares Scale factor. The Least Squares Scale Factor was: 0.644650. It is assumed that the gyro Angle Random Walk contribution is captured with the Least Squares scaling. The gyro ARW contribution can be approximately calculated as 0.0734 arcseconds, given that ARW = 100 $\mu\text{deg}/\sqrt{\text{hr}}$, with 7.481000e+002 second Maneuver time (max), and 10 independent Maneuvres.

²Gyro Scale Factor(GSF) assumes 95 ppm error over 0.250 degree maneuver.

³This can be interpreted as estimate of ”pixel to sky” pointing reconstruction error if no science data is used.

⁴This can be interpreted as estimate of achieved S/I centroiding error

IPF BROWN ANGLE SUMMARY					
FRAME TABLE USED: BodyFrames_FTU_13Aa					
NF	NAME	WAS	IS	CHANGE	UNIT
118	theta_Y	+7.061440	+7.099572	+0.038132	arcmin
118	theta_Z	-6.809500	-6.806934	+0.002566	arcmin
118	angle	-7.187501	-8.332868	-1.145367	deg
119	theta_Y	+6.423600	+6.469337	+0.045737	arcmin
119	theta_Z	-6.809500	-6.721118	+0.088382	arcmin
119	angle	-7.187500	-8.332868	-1.145368	deg
120	theta_Y	+7.157230	+7.366224	+0.208994	arcmin
120	theta_Z	-2.135771	-2.044227	+0.091544	arcmin
120	angle	-7.187501	-8.332868	-1.145367	deg
124	theta_Y	+6.596785	+6.595486	-0.001299	arcmin
124	theta_Z	-6.959165	-6.956432	+0.002733	arcmin
124	angle	-7.187501	-8.332868	-1.145367	deg
127	theta_Y	+6.296100	+6.343290	+0.047190	arcmin
127	theta_Z	-6.809500	-6.703954	+0.105546	arcmin
127	angle	-7.187500	-8.332868	-1.145368	deg
117	theta_Y	+5.396307	+6.385306	+0.988999	arcmin
117	theta_Z	-8.948538	-6.709675	+2.238863	arcmin
117	angle	+0.000049	-8.332868	-8.332917	deg

Table 1.6: IPF Brown angle summary

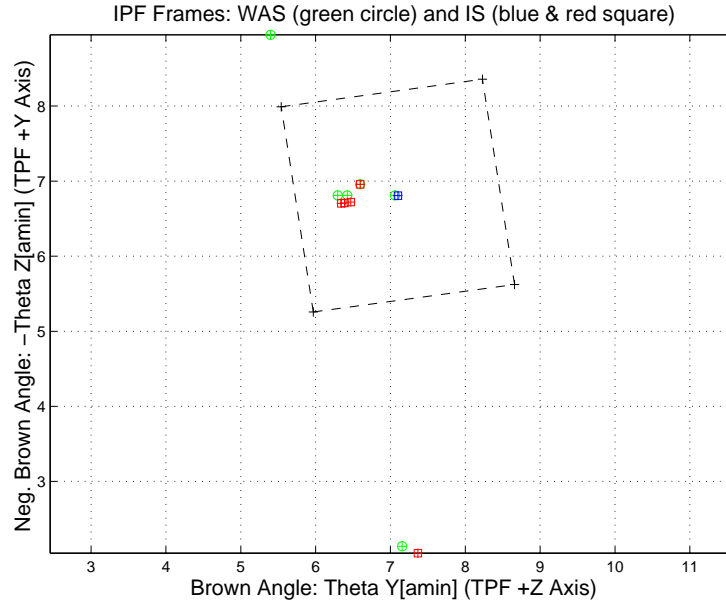


Figure 1.2: A-priori and a-posteriori IPF frames (ZOOMED)

2 IPF INPUT FILE HISTORY

STATUS	FILENAME	START TIME	END TIME
WAS	AA101118	751362000.4	751371000.3
IS	AA101118	751362000.4	751371000.3
WAS	CA201118	751363085.5	751370226.5
IS	CA201118	751363085.5	751370226.5
WAS	CB102118	751362914.9	751370020.7
IS	CB103118	751362914.9	751370020.7

Table 2.1: IPF input file begin and end times

WAS	SIZE	IS	SIZE	REMOVED	PATCHED
AA101118	90000	AA101118	90000	0	0
CA201118	180	CA201118	180	0	N/A
CB102118	85	CB103118	82	3	N/A

Table 2.2: IPF input file editing status

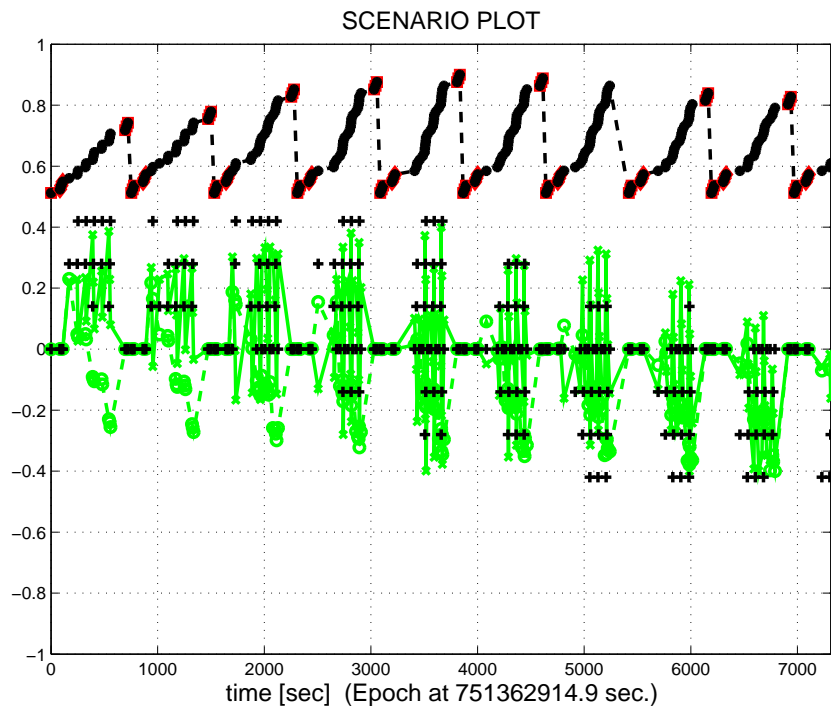


Figure 2.1: Scenario Plot

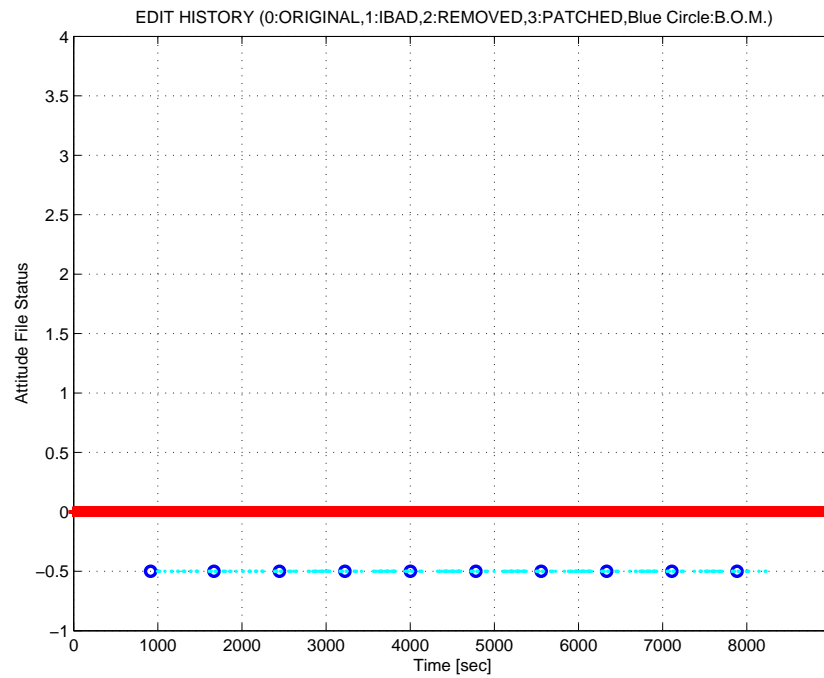


Figure 2.2: Attitude file edit history

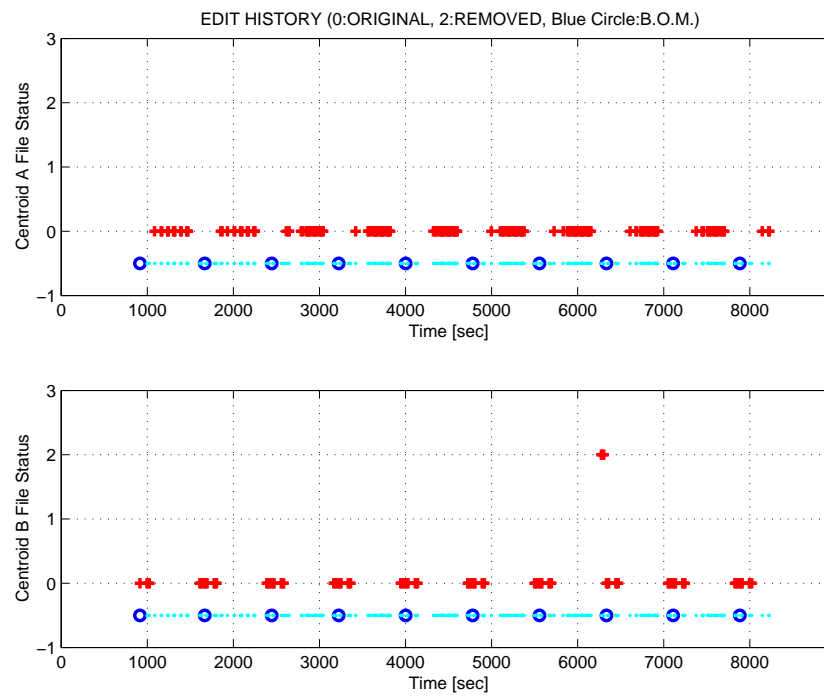


Figure 2.3: Centroid file edit history

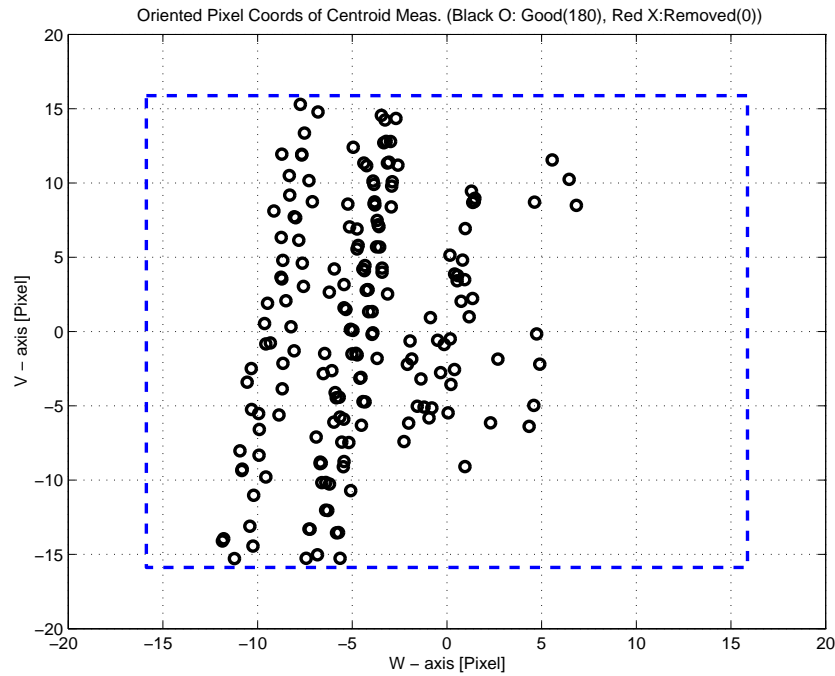


Figure 2.4: Oriented Pixel Coords of Centroid Meas. Edited Centroids

LIST OF REMOVED SCIENCE CENTROIDS

Table 2.3: List of Removed Centroids (Original CA File Row Index)

LIST OF REMOVED PCRS CENTROIDS							
59	60	61					

Table 2.4: List of Removed PCRS Centroids (Original CB File Row Index)

3 IPF EXECUTION RESULTS

3.1 IPF EXECUTION OUTPUT PLOTS

This subsection summarizes the IPF filter results. As shown in Table 3.1, the output plots are segmented to three groups: predicted performance, post-run results and IPF trending plots.

FIGURE NO.	DESCRIPTION
Predicted performance prior to IPF run	
Figure 3.1	Meas. and a-priori predicts in TPF coords
Figure 3.2	Meas. and a-priori predicts in Oriented Pixel Coords including rectangular array boundary approximation
Figure 3.3	A-Priori Prediction Error Quiver Plot in Oriented Pixel Coords including rectangular array boundary approximation
Figure 3.4	A-priori prediction error
Figure 3.5	Oriented Pixel Coords of measurements and a-priori predicts (PCRS only)
Figure 3.6	Oriented Pixel Coords of measurements and a-priori predicts (Zoomed, PCRS only)
Figure 3.7	Oriented (W,V) Pixel Coords of A-Priori PCRS Prediction Error Quiver Plot
Figure 3.8	A-priori PCRS prediction error
IPF filter performance (post run results)	
Figure 3.9	IPF execution convergence, chart 1: (top) normalized residual error vs. iteration number and (bottom) norm of effective parameter corrections
Figure 3.10	IPF execution convergence, chart 2: parameter correction size vs. iteration number
Figure 3.11	Parameter uncertainty convergence: square-root of diagonal elements of covariance matrix vs. maneuver number
Figure 3.12	IPF parameter symbol table
Figure 3.13	KF parameter error sigma plot (a-priori-dashed, a-posteriori-solid). Includes true parameter errors (FLUTE runs only)
Figure 3.14	LS parameter error sigma plot. Includes true parameter errors (FLUTE runs only)
Figure 3.15	KF and LS parameter errors sigma plot (Figure 3.13 & Figure 3.14 combined)
Figure 3.16	Measurements and a-posteriori predicts in Oriented Pixel Coords including rectangular array boundaries (a-priori-dashed, a-posteriori-solid)
Figure 3.17	Attitude corrected meas. and a-posteriori predicts in Oriented Pixel Coords including rectangular array boundaries (a-priori-dashed, a-posteriori-solid)

Table 3.1: Table of figures I (IPF run)

FIGURE NO.	DESCRIPTION
IPF filter performance (post run results) - CONTINUE	
Figure 3.18	KF innovations with (o) and w/o (+) attitude corrections
Figure 3.19	Histograms of science a-posteriori residuals (or innovations)
Figure 3.20	A-Posteriori Science Centroid Prediction Error Quiver (Att. Cor.)
Figure 3.21	Normalized A-Posteriori Science Centroid Prediction Errors
Figure 3.22	KF innovations with (o) and w/o (+) attitude corrections (PCRS)
Figure 3.23	Histograms of PCRS a-posteriori residuals (or innovations)
Figure 3.24	A-posteriori PCRS Prediction Summary
Figure 3.25	A-posteriori PCRS Prediction (PCRS 1 Only)
Figure 3.26	A-posteriori PCRS Prediction (PCRS 2 Only)
Figure 3.27	A-Posteriori PCRS Prediction Errors Quiver (Att. Cor.)
Figure 3.28	Normalized A-Posteriori PCRS Prediction Errors
Figure 3.29	W-axis KF innovations and 1-sigma bound
Figure 3.30	V-axis KF innovations and 1-sigma bound
Figure 3.31	Array plot with (solid) and w/o (dashed) optical distortion corrections
Figure 3.32	Optical Distortion Plot: total (x5 magnification)
Figure 3.33	Optical Distortion Plot: constant plate scales (x5 magnification)
Figure 3.34	Optical Distortion Plot: linear plate scale (x5 magnification)
Figure 3.35	Optical Distortion Plot: gamma terms (x5 magnification)
Figure 3.36	Scan Mirror Chops
Figure 3.37	IPF Frame Reconstruction
Figure 3.38	Center Pixel Reconstruction
IPF parameter trending plots	
Figure 3.39	Estimated attitude corrections (Body frame)
Figure 3.40	Estimated attitude error sigma plot (Body frame)
Figure 3.41	Systematic error attributed to thermo-mechanical boresight drift (equiv. angle in (W,V) coords)
Figure 3.42	Systematic error attributed to thermo-mechanical boresight drift (equiv. angle in Body frame)
Figure 3.43	Systematic error attributed to gyro drift bias (equiv. rate in (W,V) coords)
Figure 3.44	Systematic error attributed to gyro drift bias (equiv. angle in (W,V) coords)
Figure 3.45	Systematic error attributed to gyro drift bias (equiv. angle in Body frame)

Table 3.2: Table of figures II (IPF run)

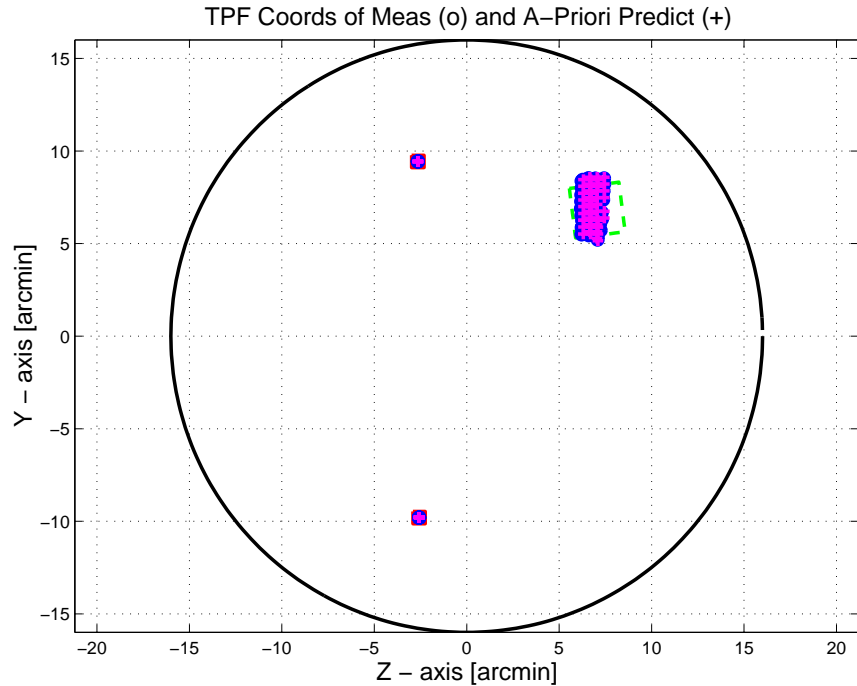


Figure 3.1: TPF coords of measurements and a-priori predicts

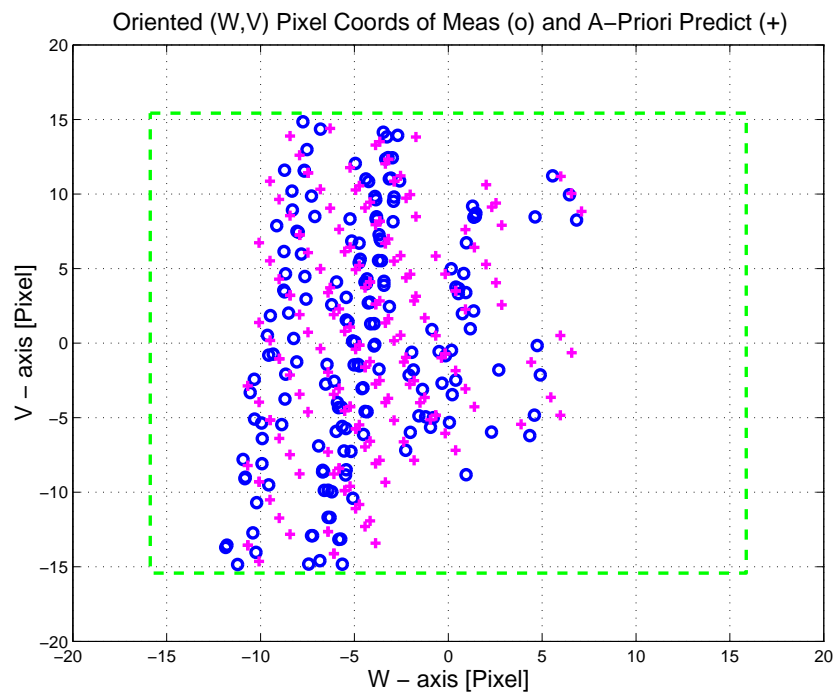


Figure 3.2: Oriented PixelCoords of measurements and a-priori predicts

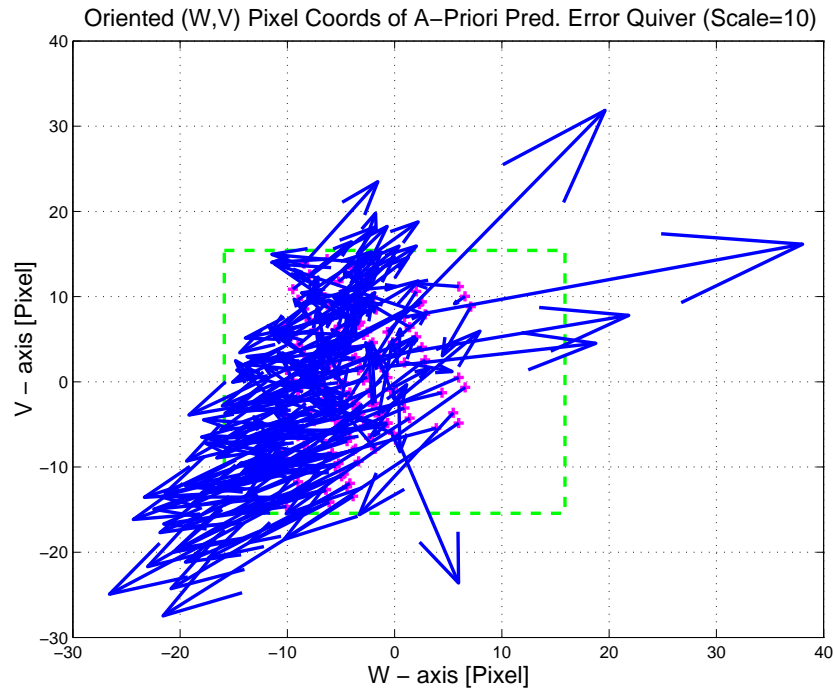


Figure 3.3: Oriented (W,V) Pixel Coords of A-Priori Prediction Error Quiver Plot

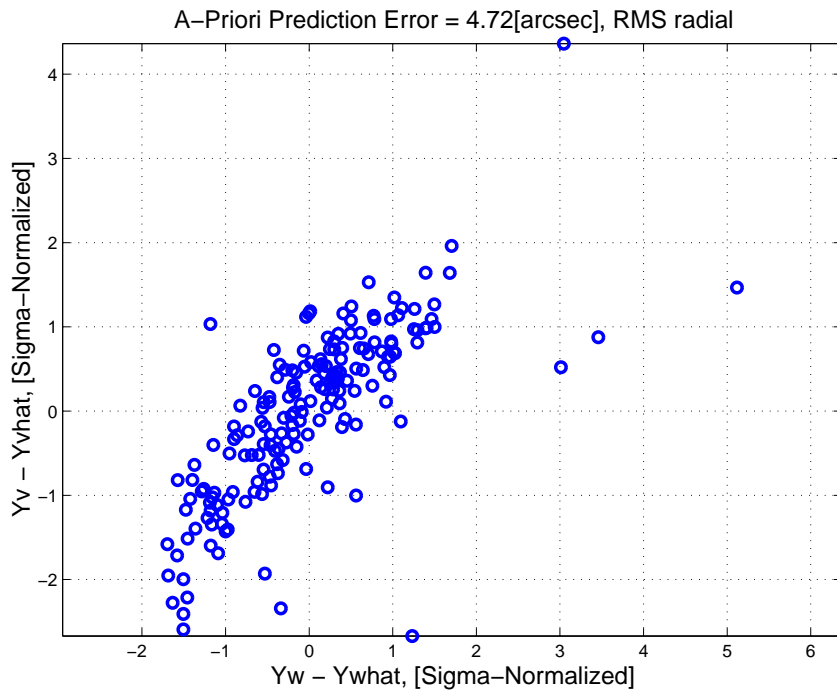


Figure 3.4: A-priori prediction error (Science Centroids)

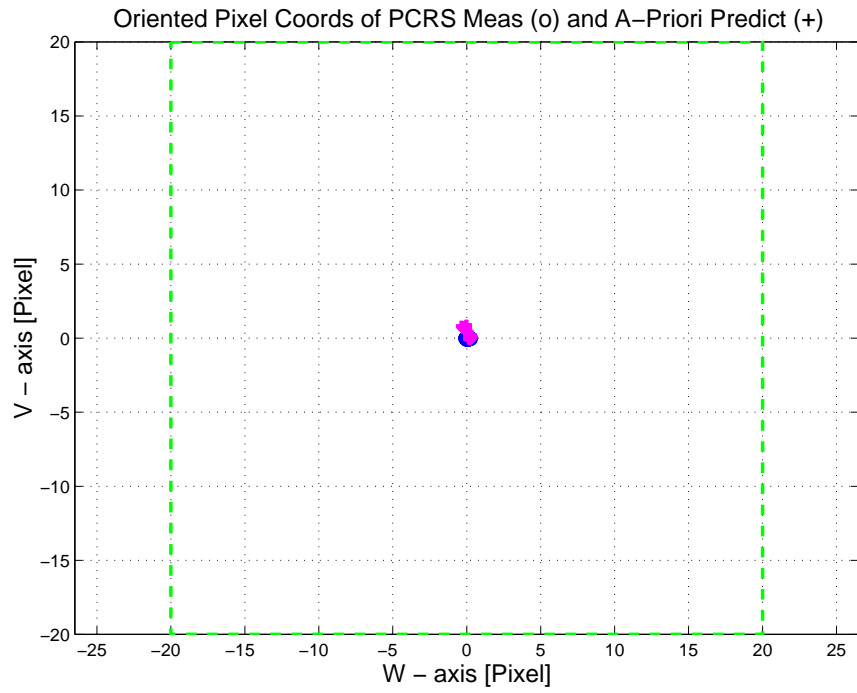


Figure 3.5: Oriented Pixel Coords of measurements and a-priori predicts (PCRS only)

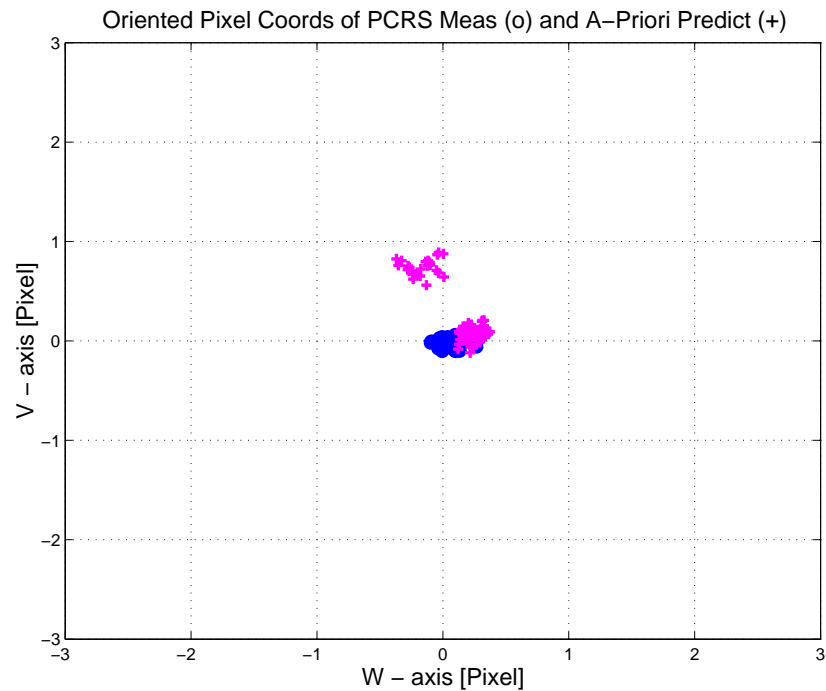


Figure 3.6: Oriented Pixel Coords of measurements and a-priori predicts (Zoomed, PCRS only)

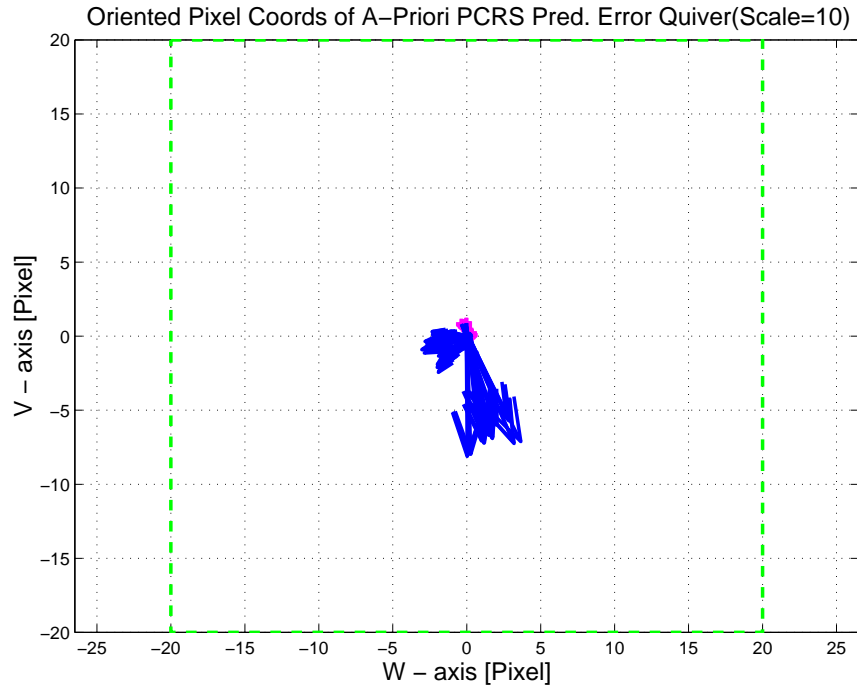


Figure 3.7: Oriented (W,V) Pixel Coords of A-Priori PCRS Prediction Error Quiver Plot

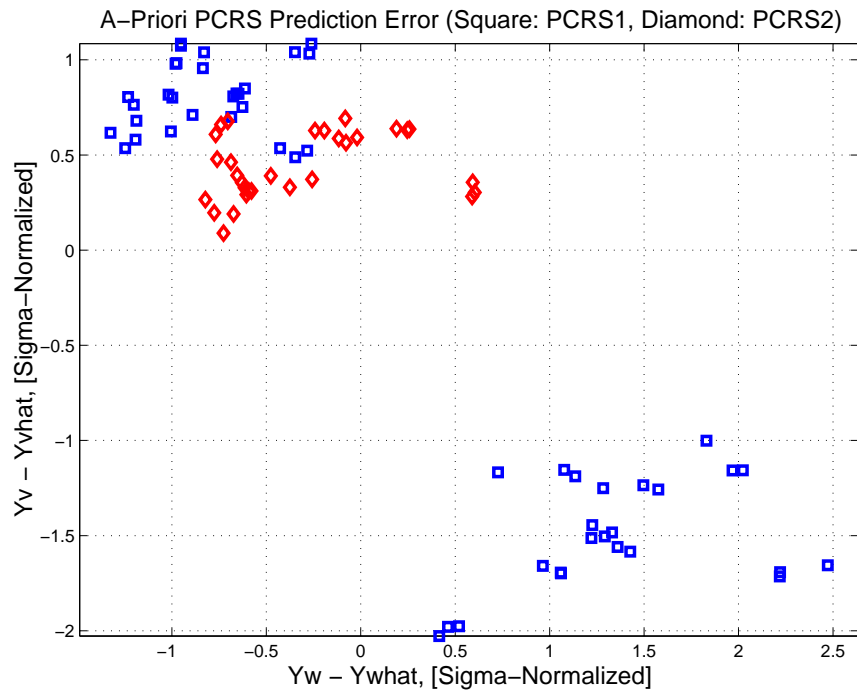


Figure 3.8: A-priori PCRS prediction error

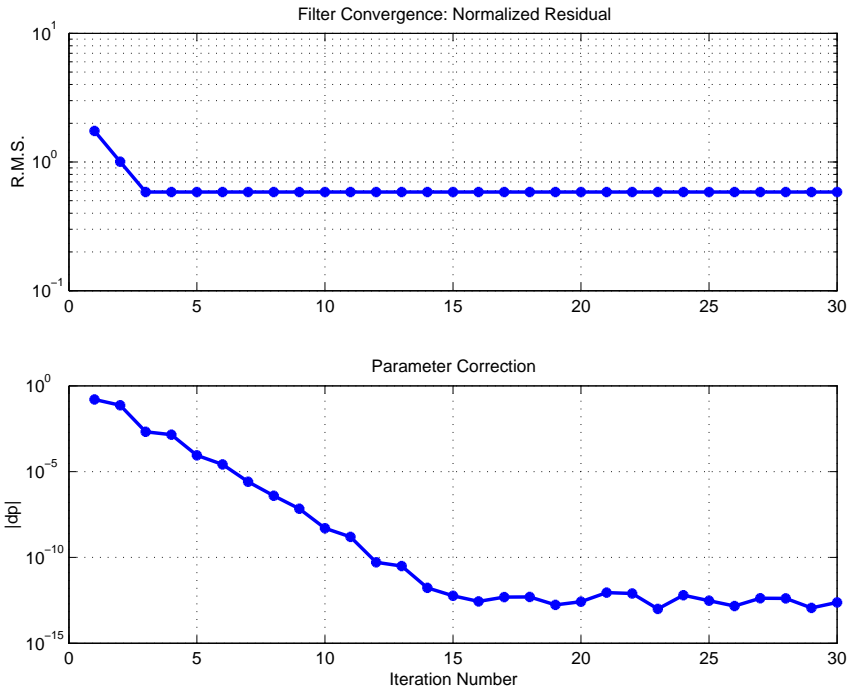


Figure 3.9: IPF execution convergence, chart 1

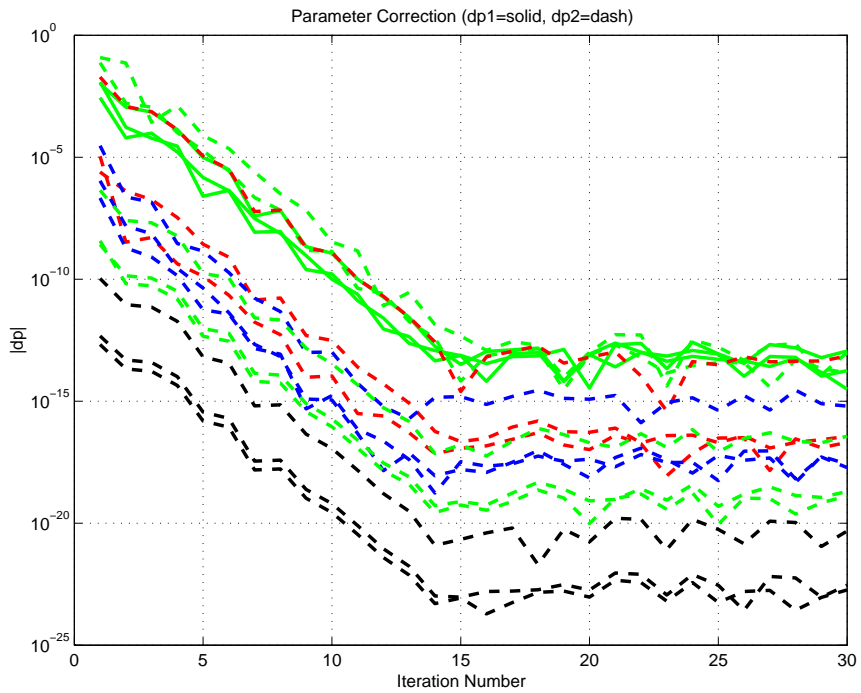


Figure 3.10: IPF execution convergence, chart 2

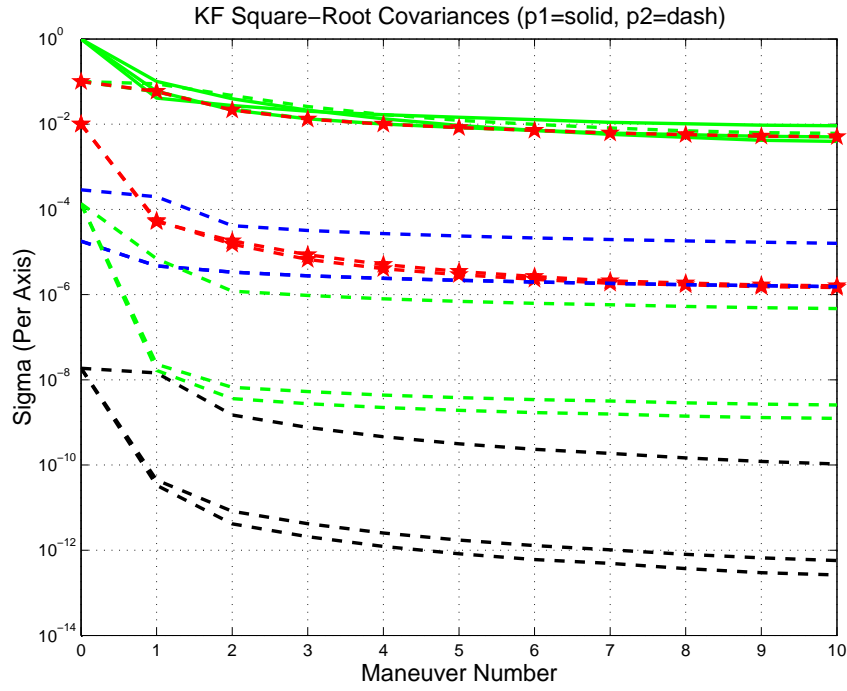


Figure 3.11: Parameter uncertainty convergence

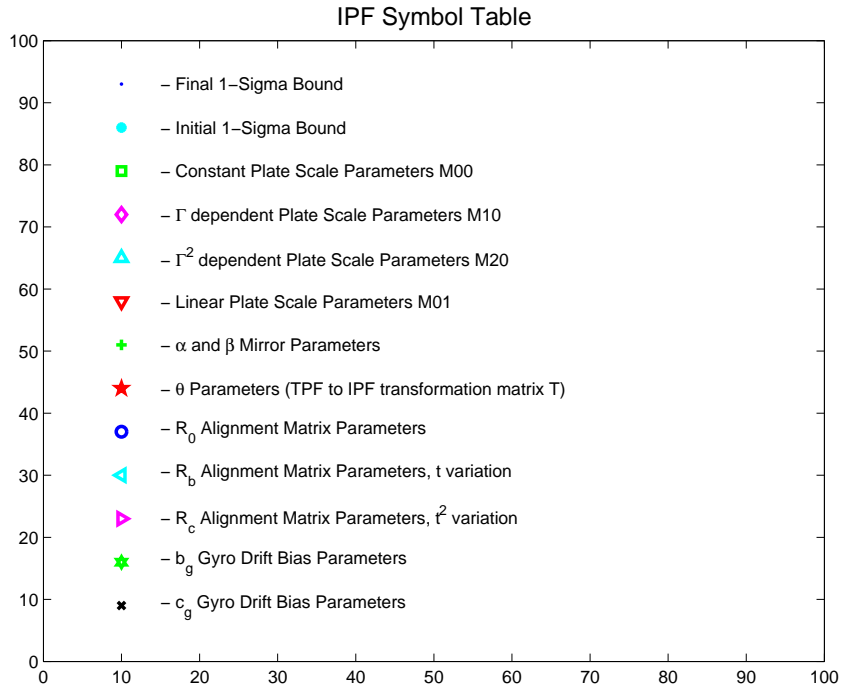


Figure 3.12: IPF parameter symbol table

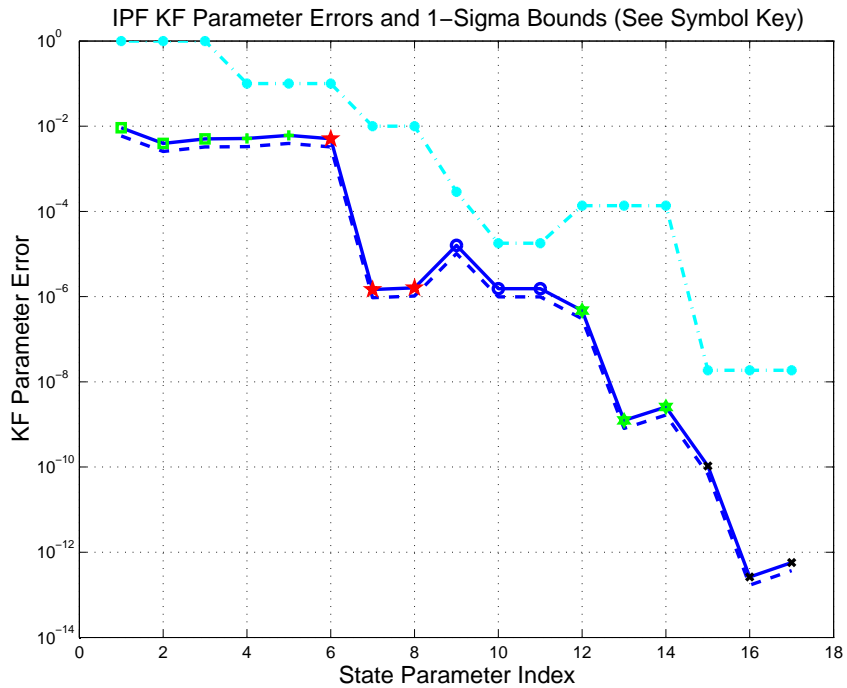


Figure 3.13: KF parameter error sigma plots

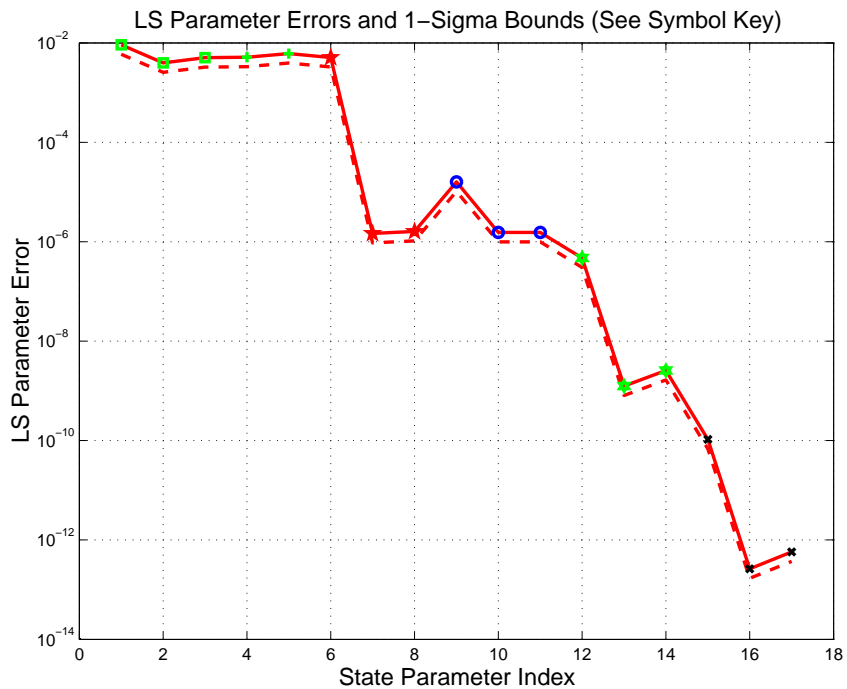


Figure 3.14: LS parameter error sigma plot

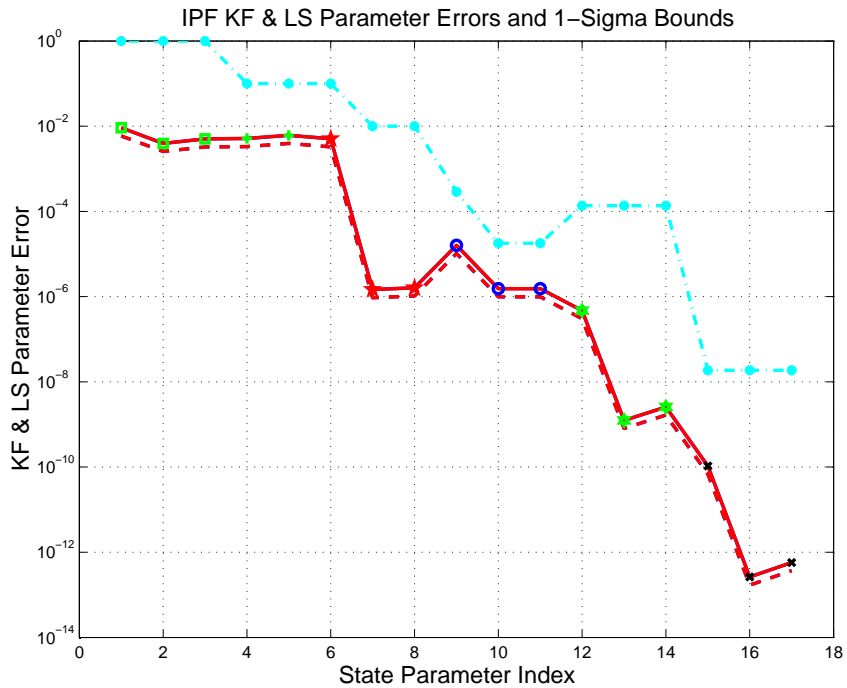


Figure 3.15: KF and LS parameter error sigma plot

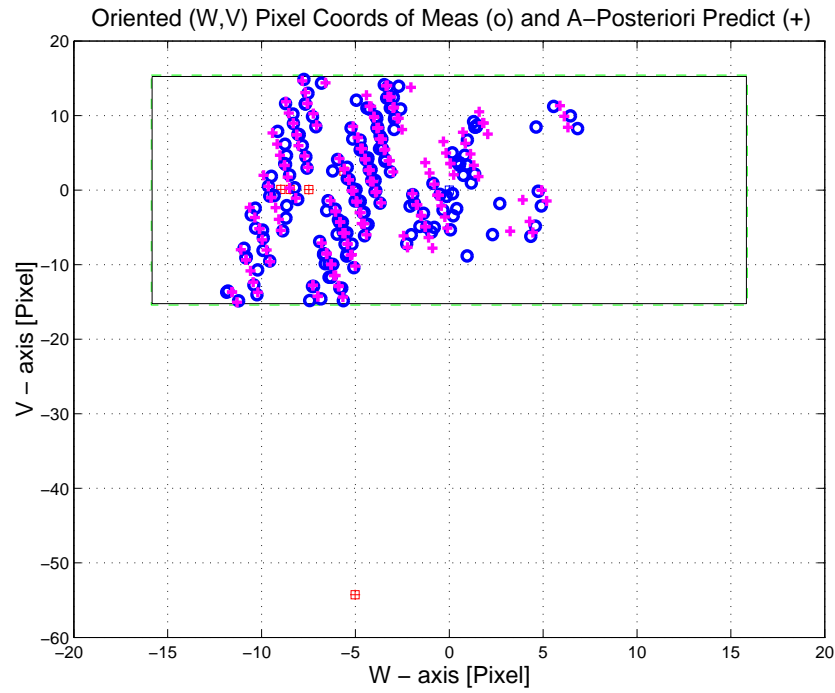


Figure 3.16: Oriented Pixel Coords of meas. and a-posteriori predicts

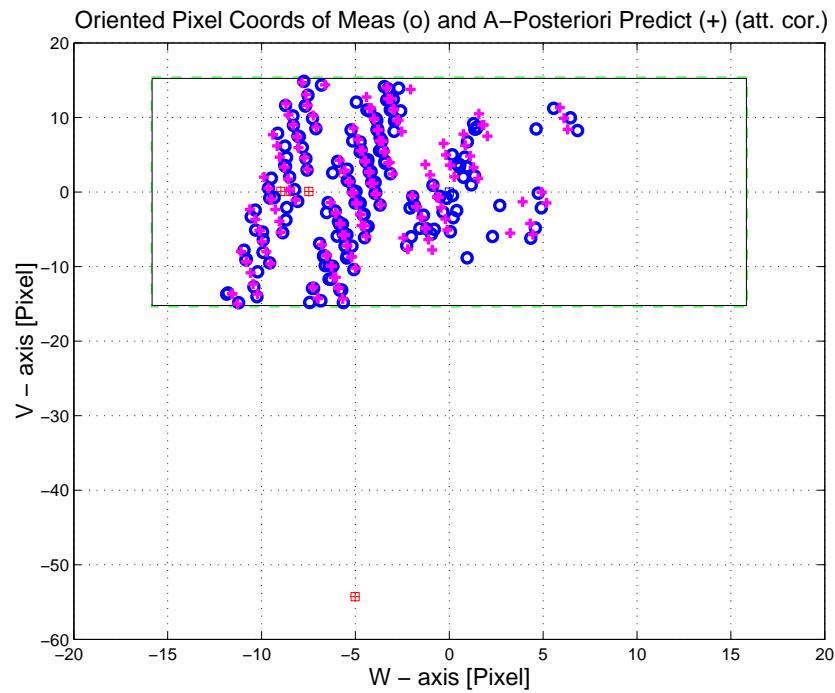


Figure 3.17: Oriented Pixel Coords of meas. and a-posteriori predicts (attitude corrected)

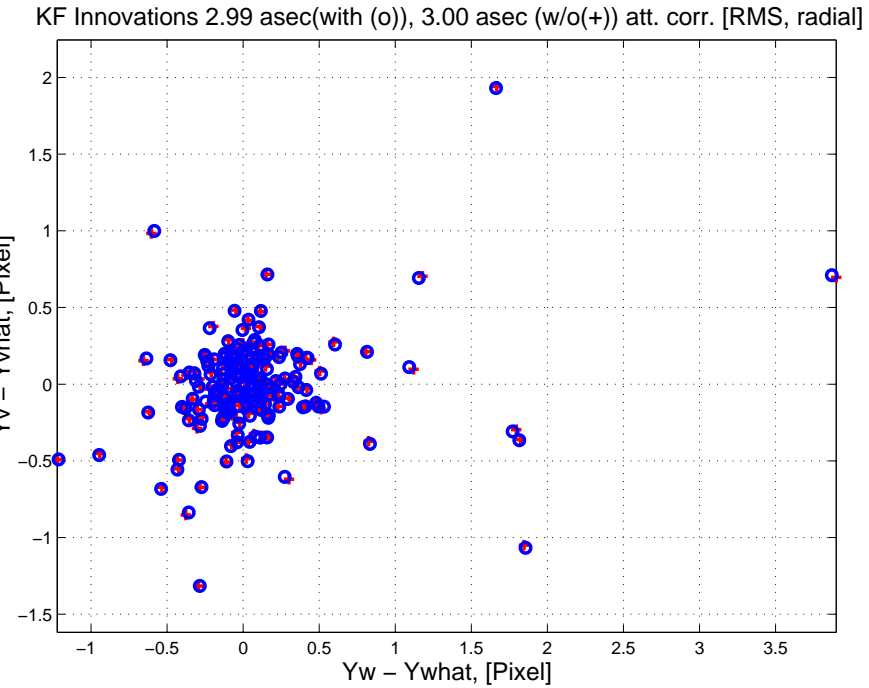


Figure 3.18: KF innovations with (o) and w/o (+) attitude corrections

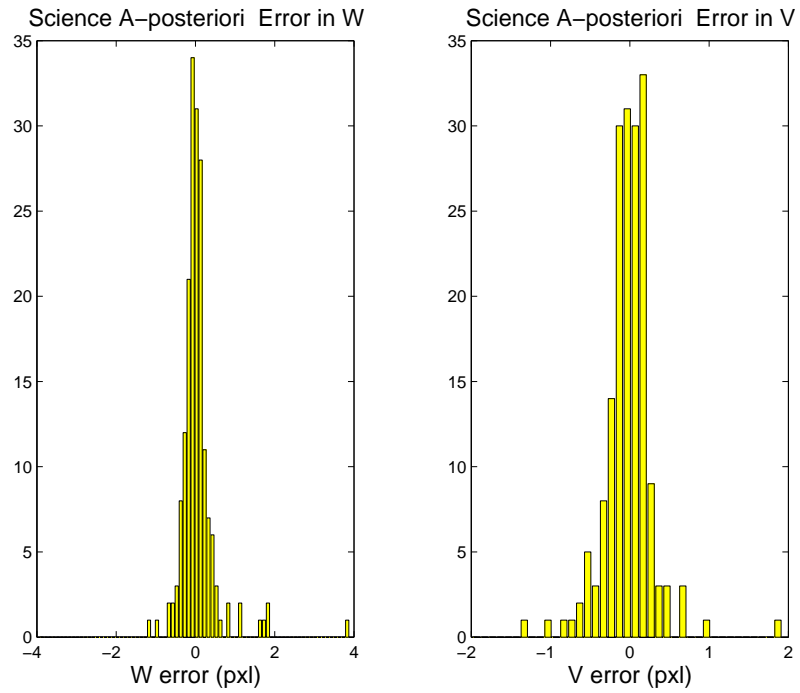


Figure 3.19: Histograms of science a-posteriori residuals (or innovations)

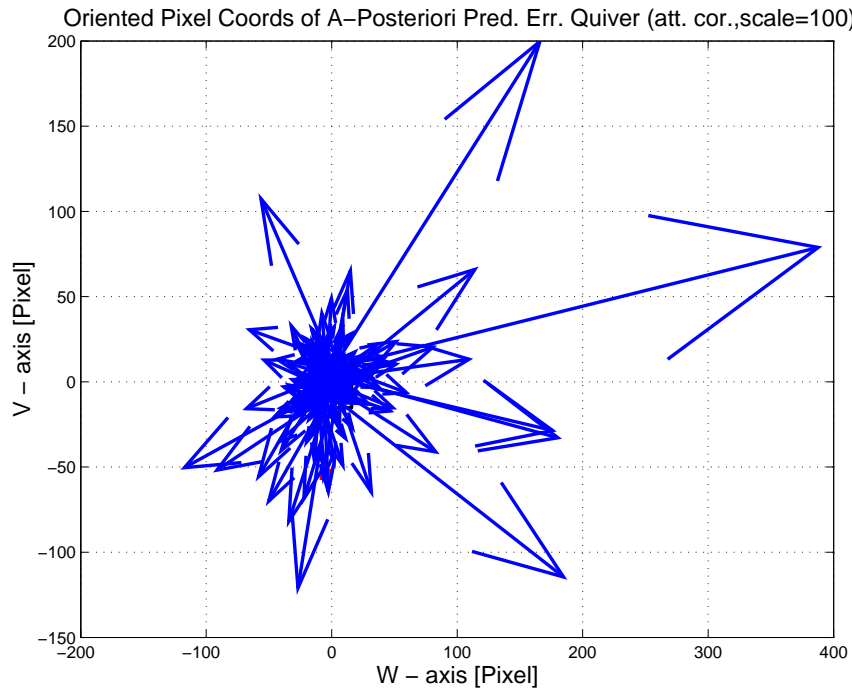


Figure 3.20: A-Posteriori Science Centroid Prediction Error Quiver (Att. Cor.)

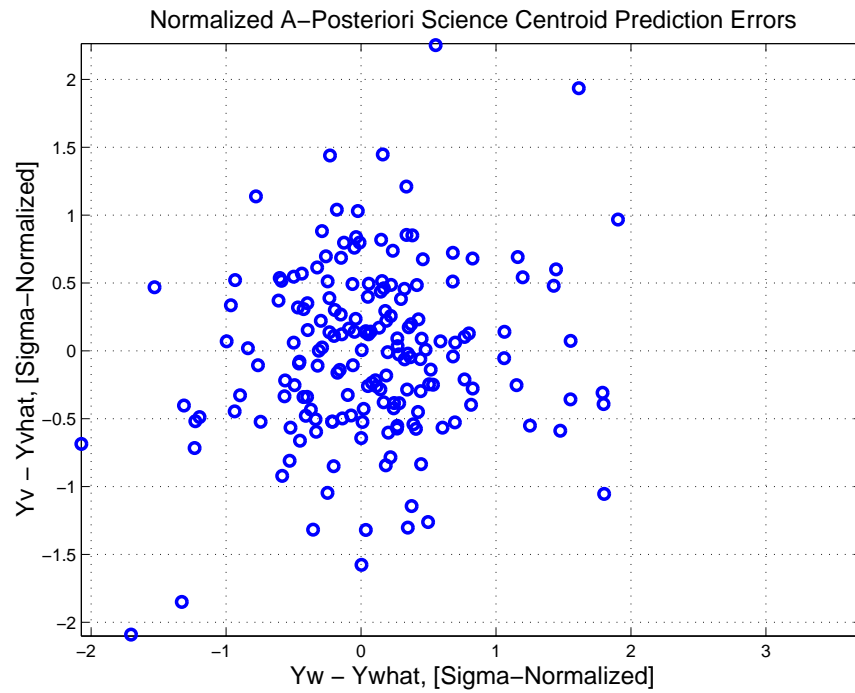


Figure 3.21: Normalized A-Posteriori Science Centroid Prediction Errors

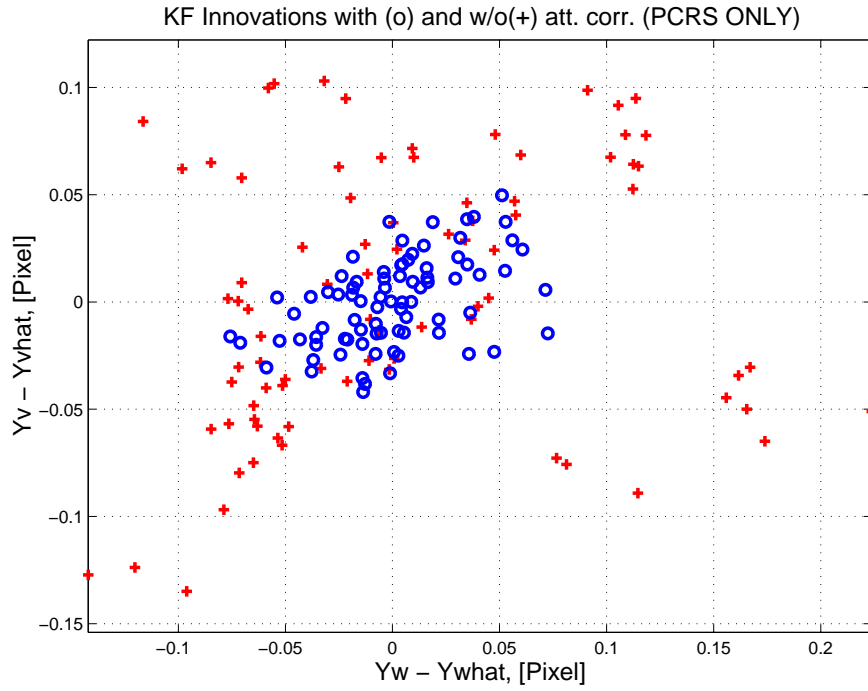


Figure 3.22: KF innovations with (o) and w/o (+) attitude corrections (PCRS)

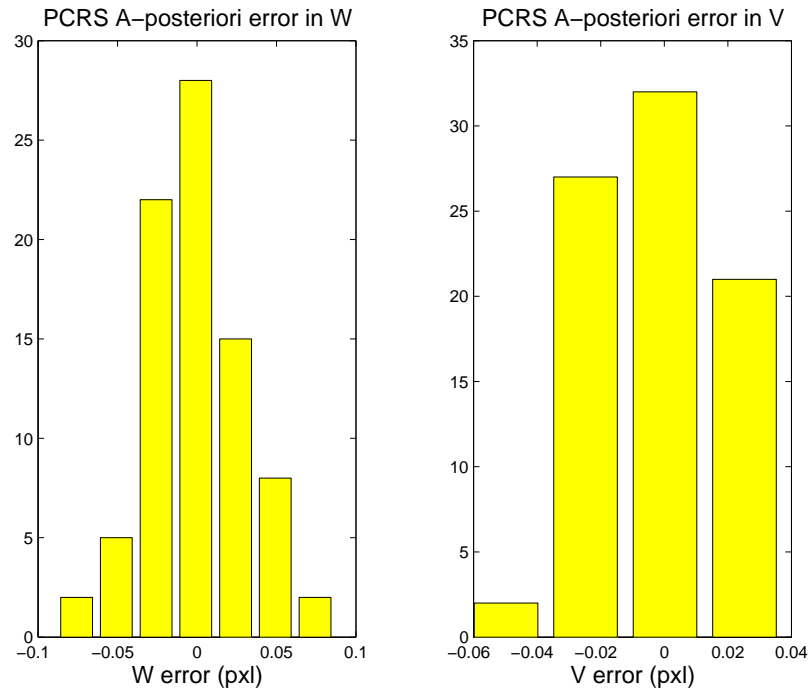


Figure 3.23: Histograms of PCRS a-posteriori residuals (or innovations)

IPF PCRS SUMMARY						
PCRS 1 (Total of 52 centroids)						
RMS	MEAN		SIGMA			
METRIC	APOST.	ATT. COR.	APOST.	ATT. COR.	STAT. CONF.	UNITS
Radial	0.0072	0.0008	0.1004	0.0418	0.0058	arcsec
W-axis	0.0057	-0.0000	0.0782	0.0364	0.0050	arcsec
V-axis	0.0045	0.0008	0.0629	0.0205	0.0028	arcsec
PCRS 2 (Total of 30 centroids)						
METRIC	APOST.	ATT. COR.	APOST.	ATT. COR.	STAT. CONF.	UNITS
Radial	0.0017	0.0016	0.1012	0.0283	0.0052	arcsec
W-axis	-0.0000	0.0000	0.0842	0.0193	0.0035	arcsec
V-axis	-0.0017	-0.0016	0.0562	0.0207	0.0038	arcsec
Combined (Total of 82 centroids)						
METRIC	APOST.	ATT. COR.	APOST.	ATT. COR.	STAT. CONF.	UNITS
Radial	0.0042	0.0001	0.1008	0.0374	0.0041	arcsec
W-axis	0.0036	-0.0000	0.0805	0.0312	0.0035	arcsec
V-axis	0.0022	-0.0001	0.0606	0.0206	0.0023	arcsec

Table 3.3: PCRS measurement prediction error summary

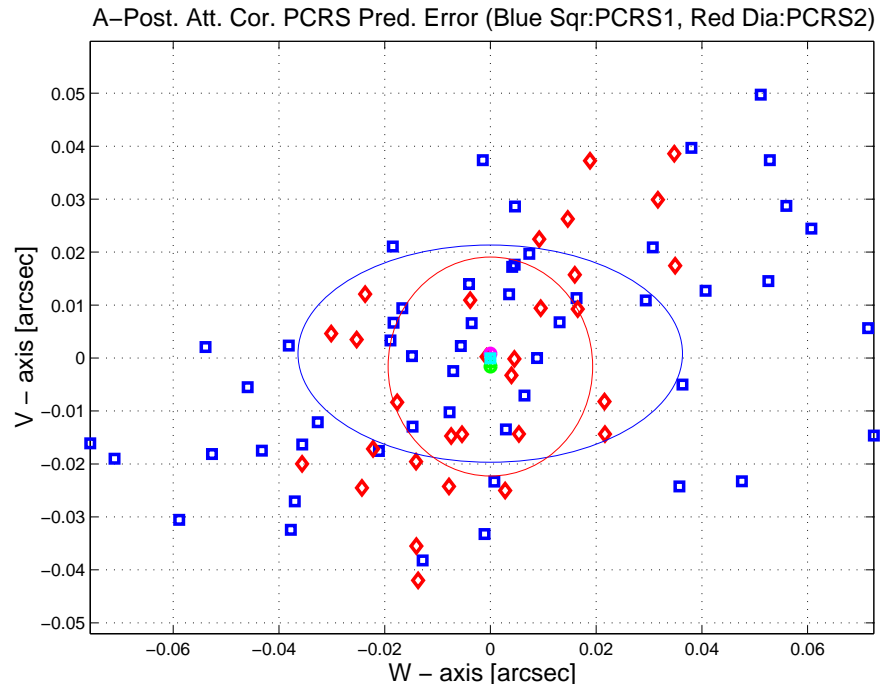


Figure 3.24: A-posteriori PCRS Prediction Summary

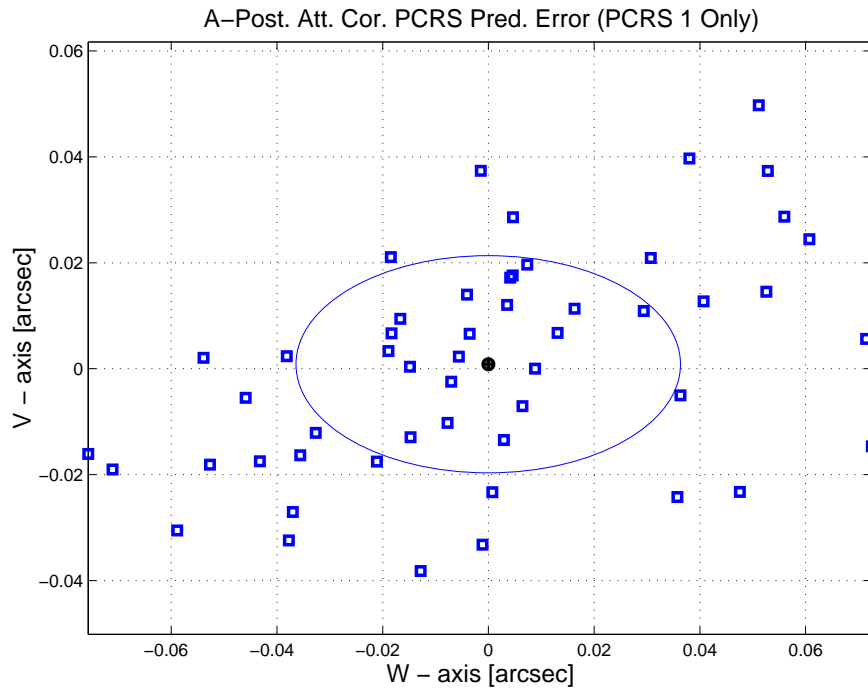


Figure 3.25: A-posteriori PCRS Prediction (PCRS 1 Only)

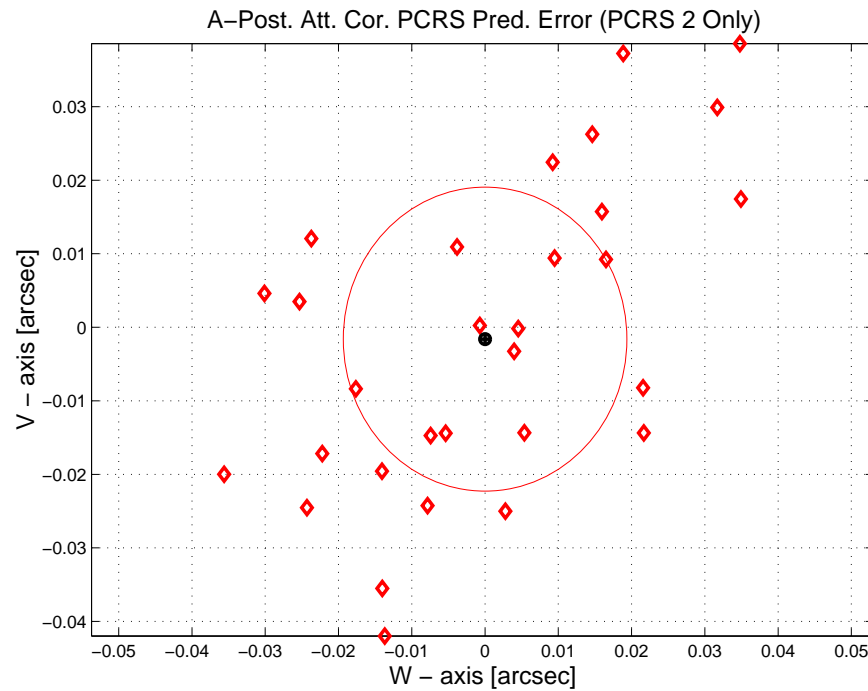


Figure 3.26: A-posteriori PCRS Prediction (PCRS 2 Only)

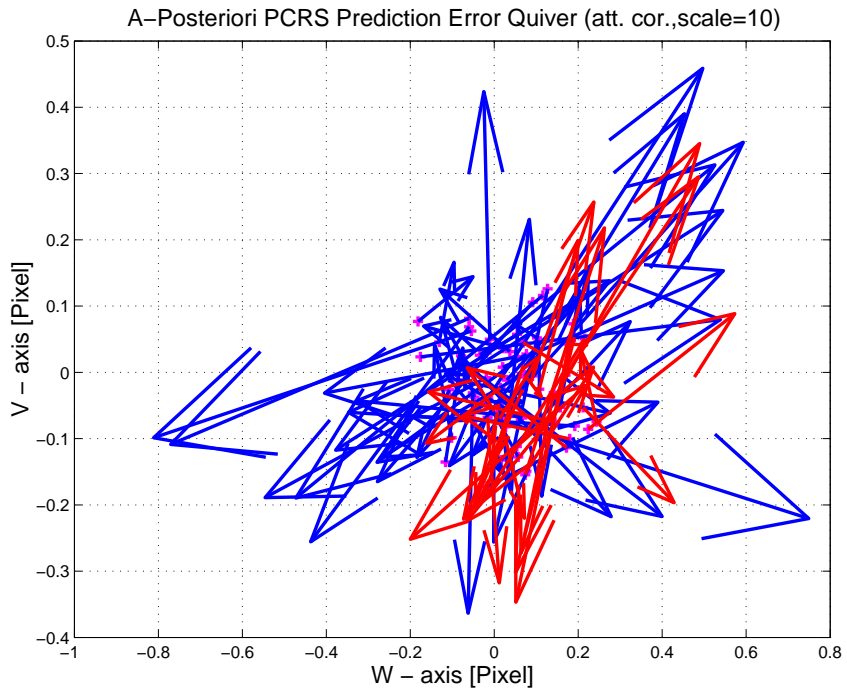


Figure 3.27: A-Posteriori PCRS Prediction Errors Quiver (Att. Cor.)

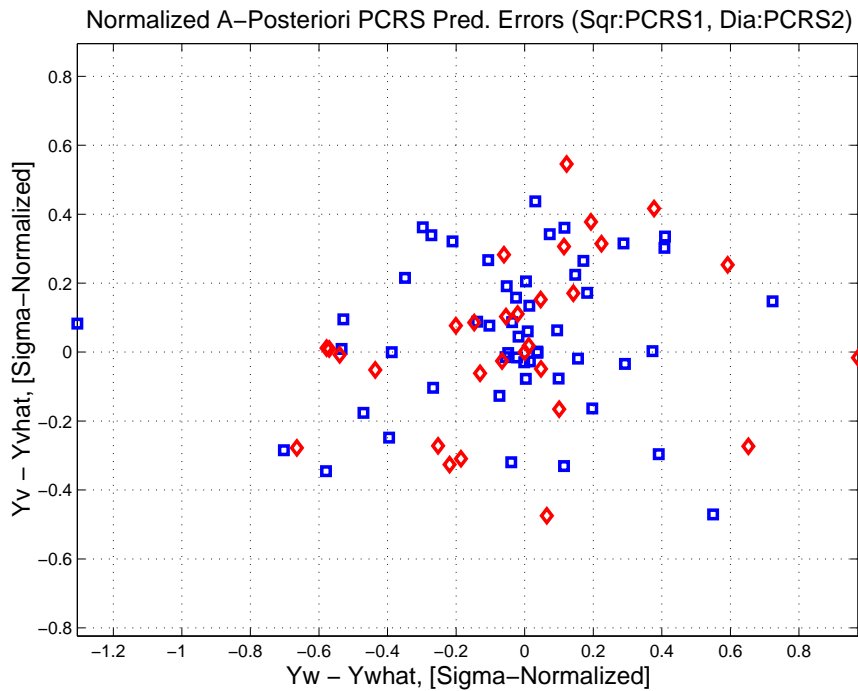


Figure 3.28: Normalized A-Posteriori PCRS Prediction Errors

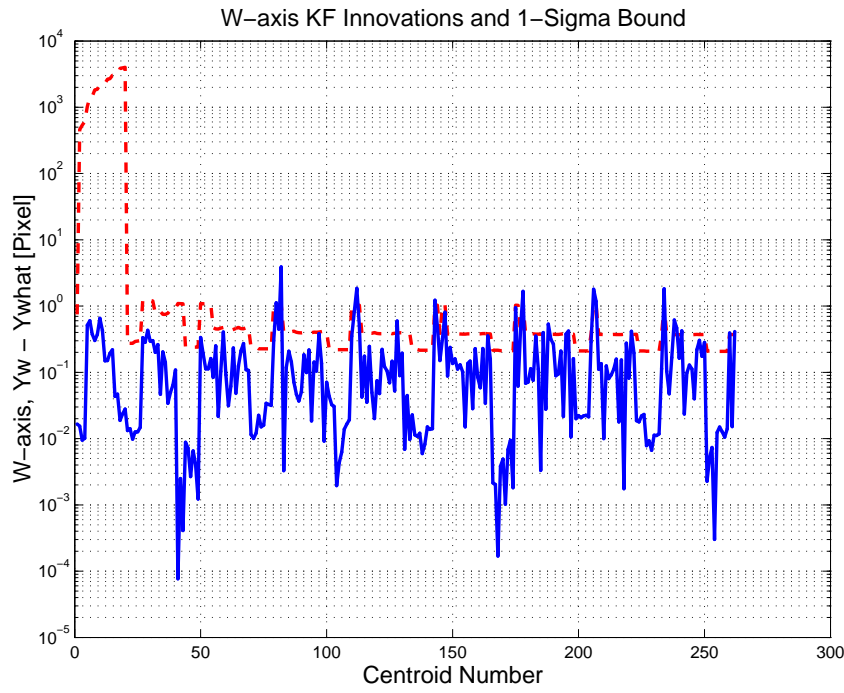


Figure 3.29: W-axis KF innovations and 1-sigma bound

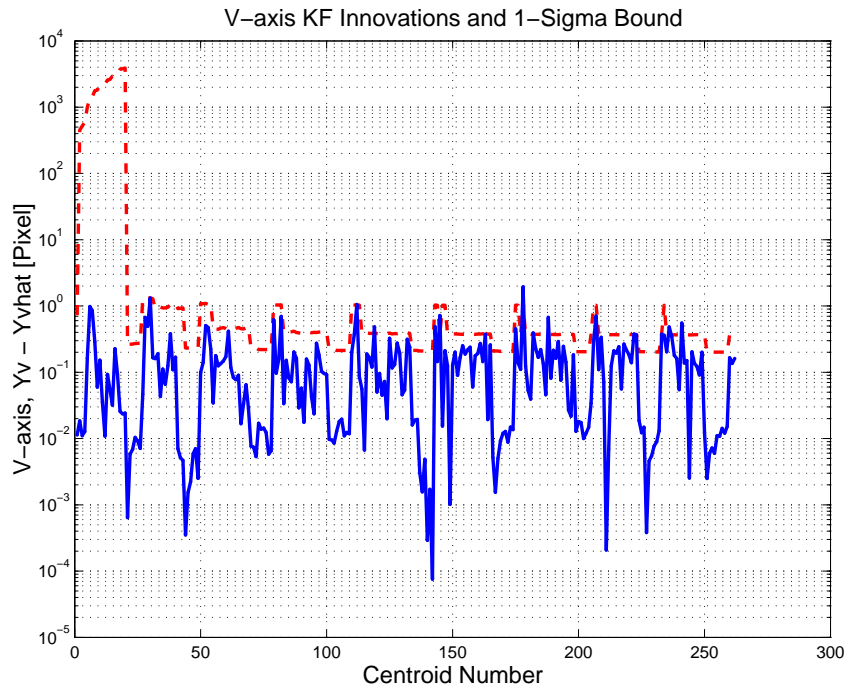


Figure 3.30: V-axis KF innovations and 1-sigma bound

S/I Array Plot with and without Optical Distortion Corrections

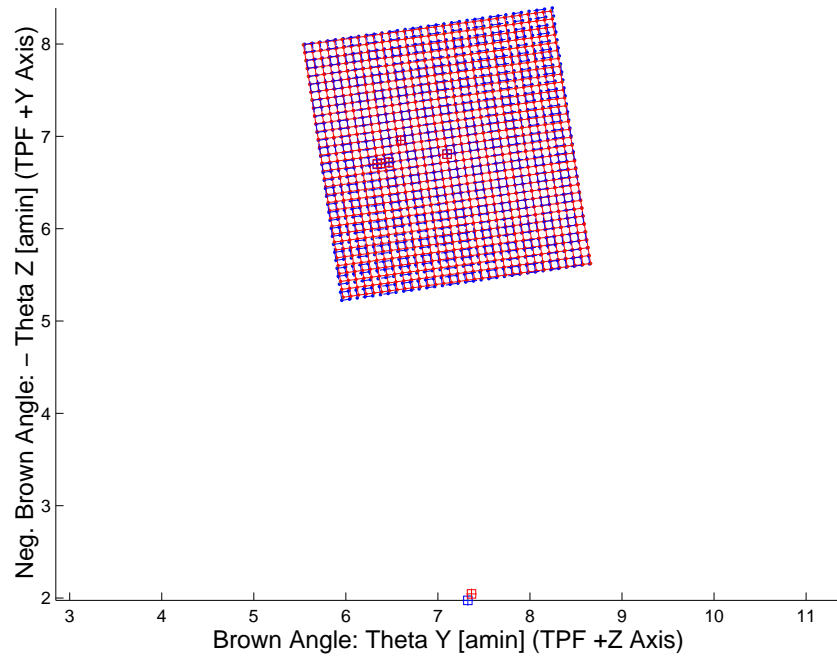


Figure 3.31: Array plot with (solid) and w/o (dashed) optical distortion corrections

Optical Distortion Plot: total (x5 magnification)

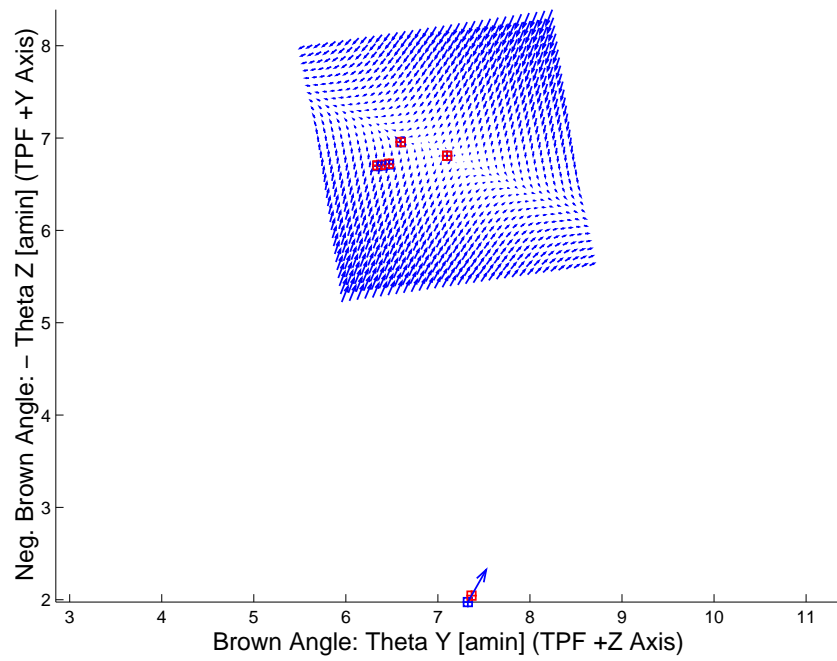


Figure 3.32: Optical Distortion Plot: total (x5 magnification)

Optical Distortion Plot: constant plate scales (x5 magnification)

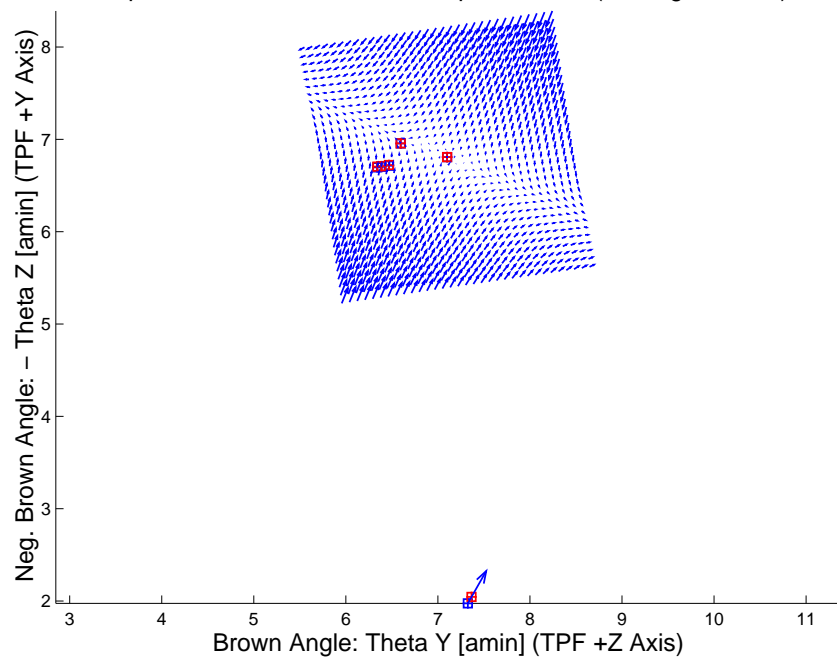


Figure 3.33: Optical Distortion Plot: constant plate scales (x5 magnification)

Optical Distortion Plot: linear plate scale (x5 magnification)

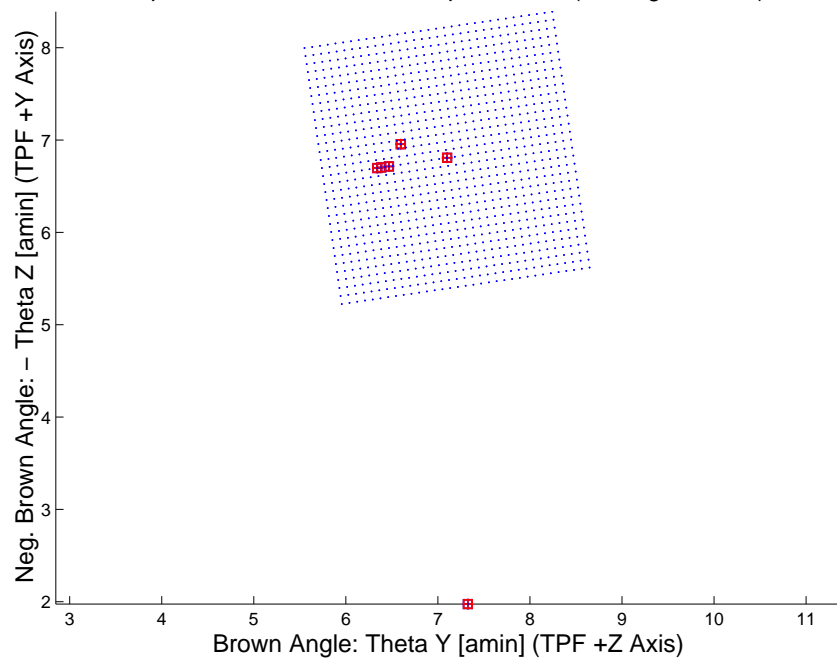


Figure 3.34: Optical Distortion Plot: linear plate scale (x5 magnification)

Opt. Dist. Plot: Γ depdt; $\Gamma = -4.08090e-004$ in blue and $\Gamma = 4.08090e-004$ in red (x5 magn)

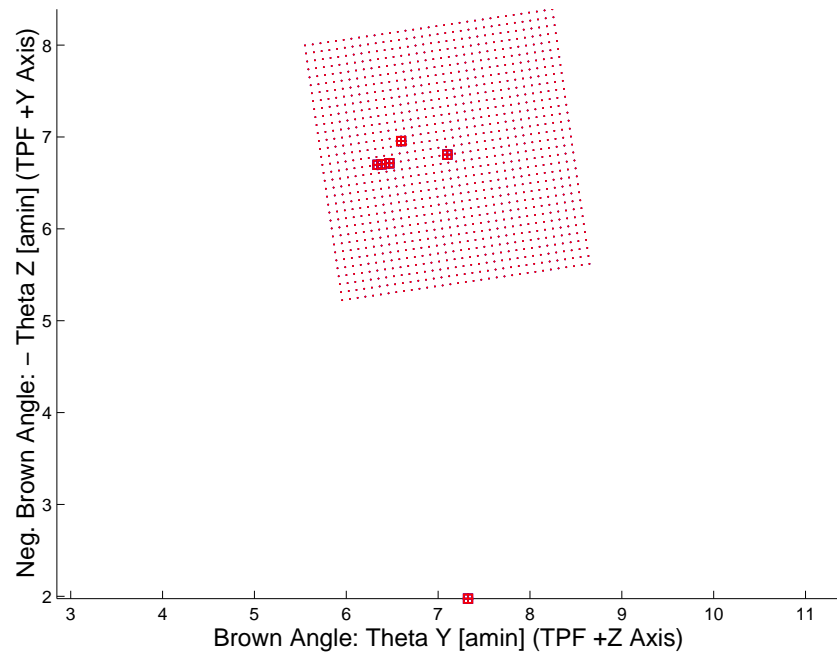


Figure 3.35: Optical Distortion Plot: gamma terms (x5 magnification)

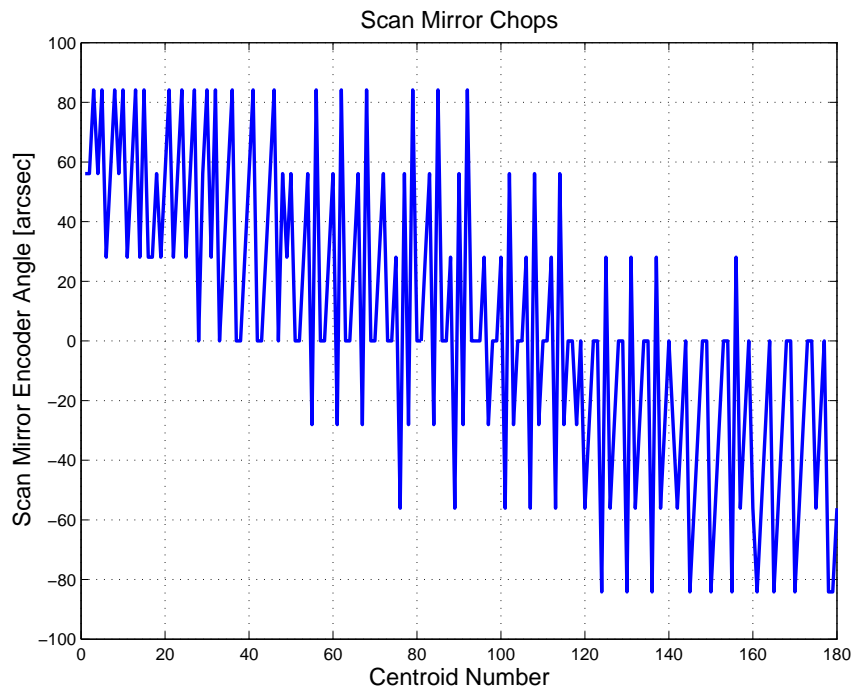


Figure 3.36: Scan Mirror Chops

IPF Frame Reconstruction (P:Blue,I(1):Green,I(2):Red,I(3):Cyan,I(4):magenta,...)

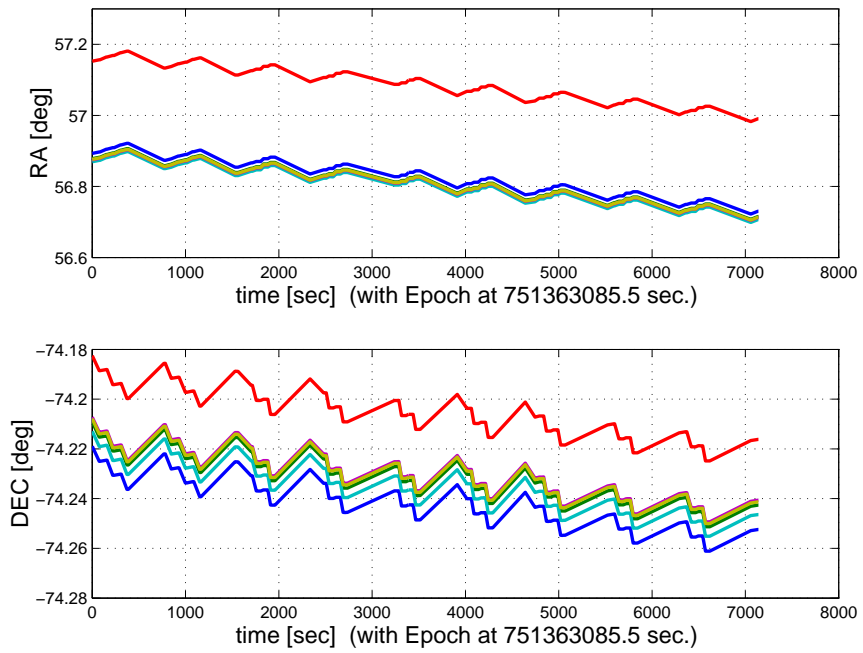


Figure 3.37: IPF Frame Reconstruction

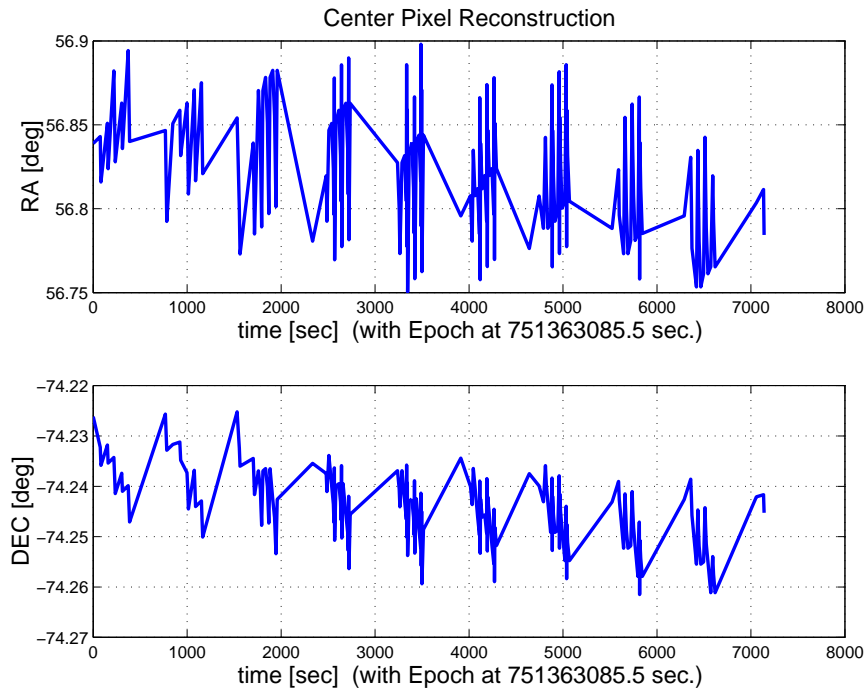


Figure 3.38: Center Pixel Reconstruction

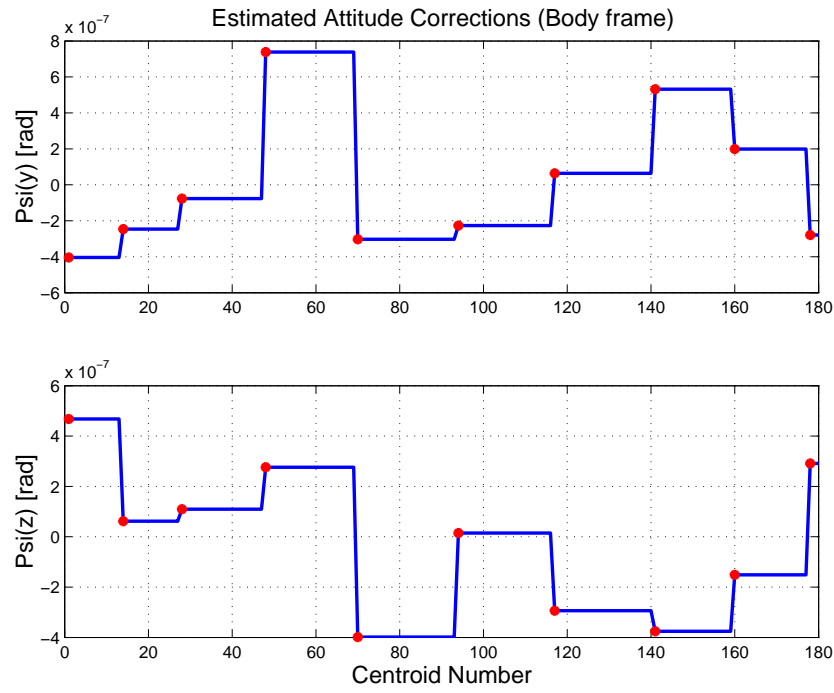


Figure 3.39: Estimated attitude corrections (Body frame)

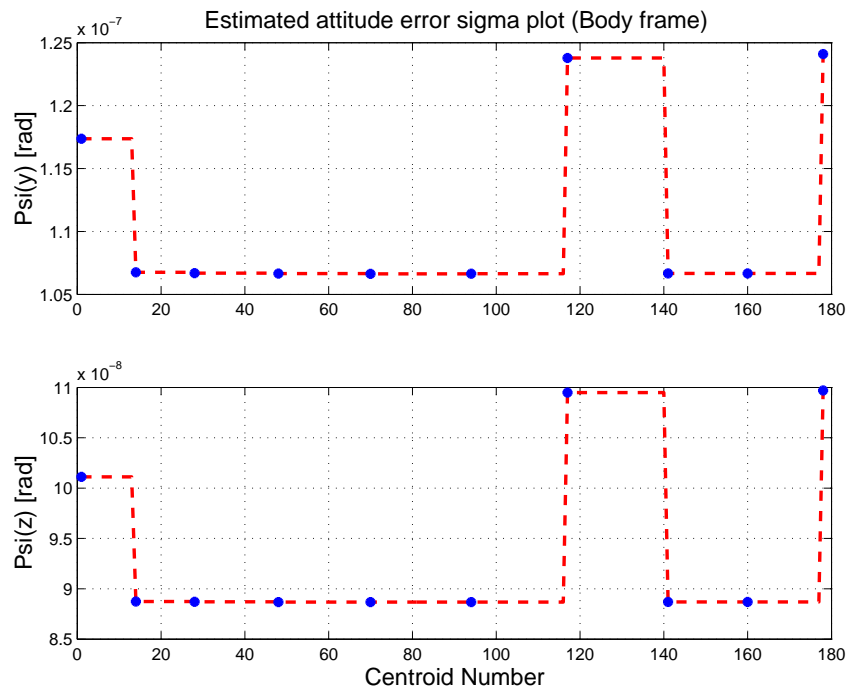


Figure 3.40: Estimated attitude error sigma plot (Body frame)

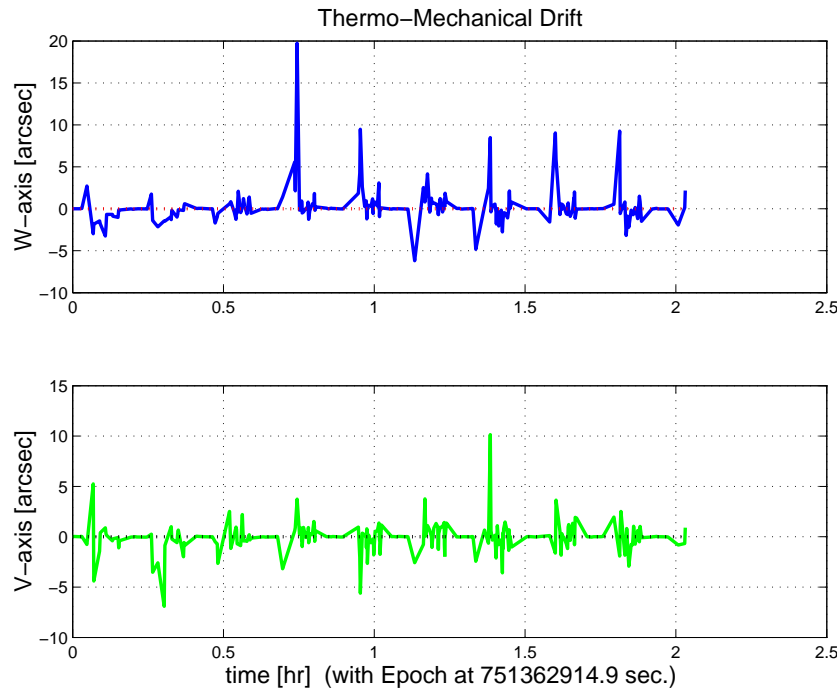


Figure 3.41: Thermo-mechanical boresight drift (equiv. angle in (W,V) coords)

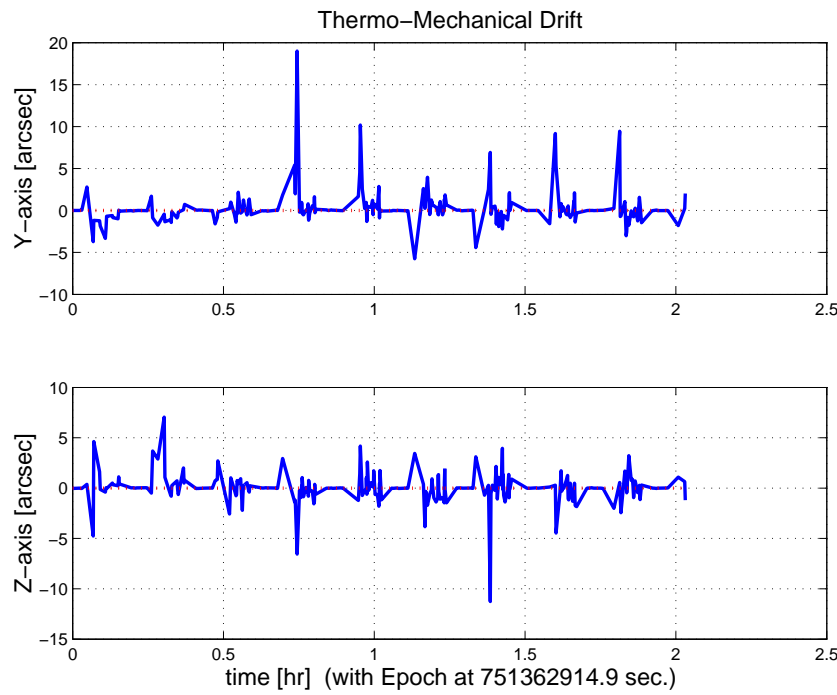


Figure 3.42: Thermo-mechanical boresight drift (equiv. angle in Body frame)

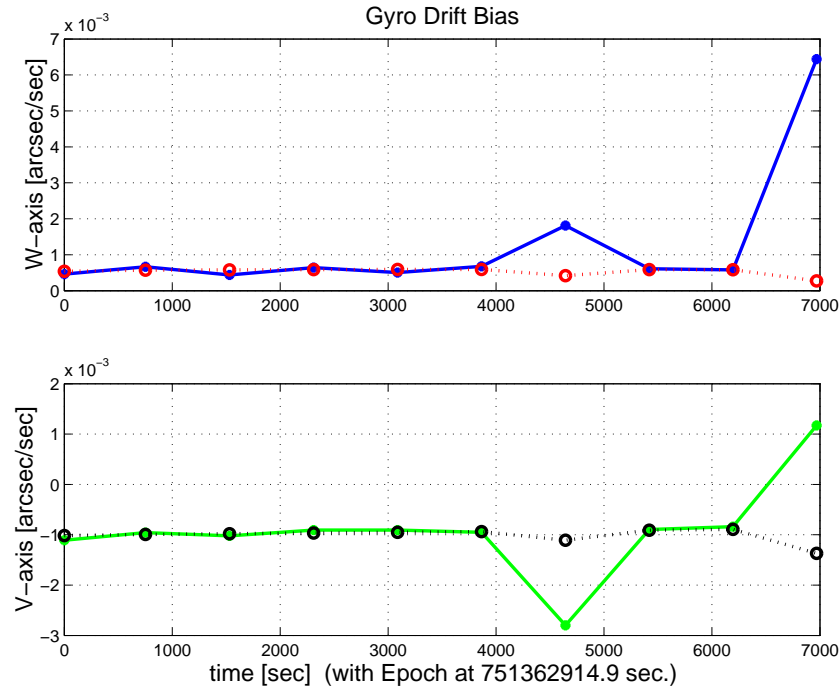


Figure 3.43: Gyro drift bias contribution (equiv. rate in (W,V) coords)



Figure 3.44: Gyro drift bias contribution (equiv. angle in (W,V) coords)

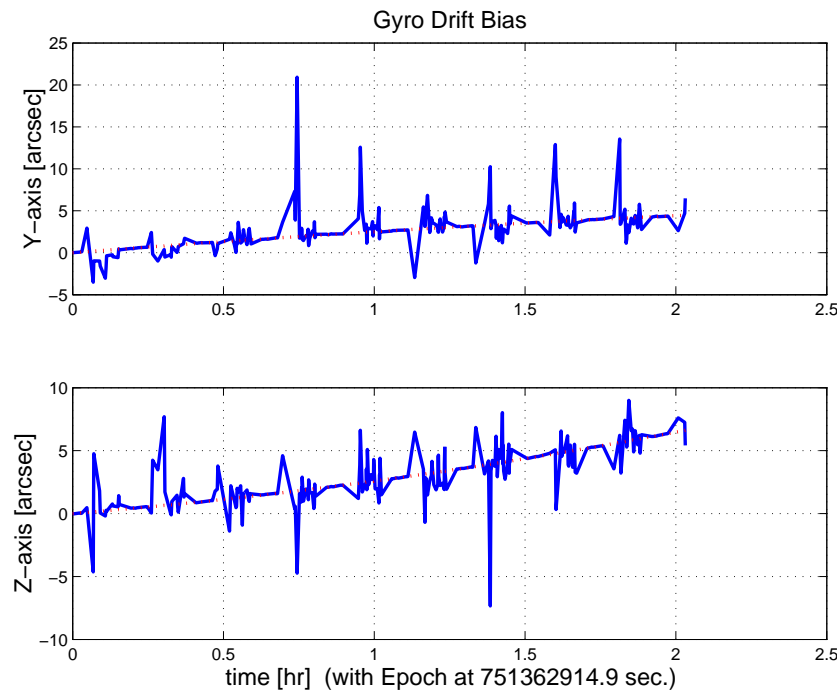


Figure 3.45: Gyro drift bias contribution (equiv. angle in Body frame)

3.2 IPF OUTPUT DATA (IF MINI FILE)

OUTPUT FILE NAME: IFmini203118.dat DATE: 20-Nov-2003 TIME: 15:54
 INSTRUMENT NAME: MIPS_70um_fine_center NF: 118
 IPF FILTER VERSION: IPF.V3.0.OB SW RELEASE DATE: November 3, 2003
 FRAME TABLE USED: BodyFrames_FTU_13Aa

IPF BROWN ANGLE SUMMARY						
Frame Number	WAS			IS		
	theta_Y (arcmin)	theta_Z (arcmin)	angle (deg)	theta_Y (arcmin)	theta_Z (arcmin)	angle (deg)
118	+7.061440	-6.809500	-7.187501	+7.099572	-6.806934	-8.332868
119	+6.423600	-6.809500	-7.187500	+6.469337	-6.721118	-8.332868
120	+7.157230	-2.135771	-7.187501	+7.366224	-2.044227	-8.332868
124	+6.596785	-6.959165	-7.187501	+6.595486	-6.956432	-8.332868
127	+6.296100	-6.809500	-7.187500	+6.343290	-6.703954	-8.332868
117	+5.396307	-8.948538	+0.000049	+6.385306	-6.709675	-8.332868
OFFSET	NF	Delta_CW	Delta_CV			
0	118	+0.000	+0.000	pixels		
OFFSET FRAME NAME: MIPS_70um_fine_center						
Brown Angle	theta_Y(arcmin)	theta_Z(arcmin)	angle(deg)			
WAS(FTB)	+7.061440	-6.809500	-7.187501			
IS (EST)	+7.099572	-6.806934	-8.332868			
dT_EST	+0.038132	+0.002566	-1.145367			
T_sSIGMA	+0.003249	+0.003553	+0.186947			
dT_EST/T_sSIGMA	+11.735822	+0.722054	-6.126690			
OFFSET	NF	Delta_CW	Delta_CV			
1	119	-7.500	+0.000	pixels		
OFFSET FRAME NAME: MIPS_70um_fine_FOV1						
Brown Angle	theta_Y(arcmin)	theta_Z(arcmin)	angle(deg)			
WAS(FTB)	+6.423600	-6.809500	-7.187500			
IS (EST)	+6.469337	-6.721118	-8.332868			
dT_EST	+0.045737	+0.088382	-1.145368			
T_sSIGMA	+0.001719	+0.002433	+0.186947			
dT_EST/T_sSIGMA	+26.599880	+36.326945	-6.126695			
OFFSET	NF	Delta_CW	Delta_CV			
2	120	-5.600	-55.000	pixels		
OFFSET FRAME NAME: MIPS_70um_fine_FOV2						
Brown Angle	theta_Y(arcmin)	theta_Z(arcmin)	angle(deg)			
WAS(FTB)	+7.157230	-2.135771	-7.187501			
IS (EST)	+7.366224	-2.044227	-8.332868			
dT_EST	+0.208994	+0.091544	-1.145367			
T_sSIGMA	+0.010881	+0.012612	+0.186947			
dT_EST/T_sSIGMA	+19.207923	+7.258332	-6.126696			
OFFSET	NF	Delta_CW	Delta_CV			
3	124	-5.600	+2.500	pixels		
OFFSET FRAME NAME: MIPS_70um_fine_FOV3						
Brown Angle	theta_Y(arcmin)	theta_Z(arcmin)	angle(deg)			
WAS(FTB)	+6.596785	-6.959165	-7.187501			
IS (EST)	+6.595486	-6.956432	-8.332868			
dT_EST	-0.001299	+0.002733	-1.145367			
T_sSIGMA	+0.001529	+0.002225	+0.186947			
dT_EST/T_sSIGMA	-0.849629	+1.228359	-6.126690			
OFFSET	NF	Delta_CW	Delta_CV			
4	127	-9.000	+0.000	pixels		
OFFSET FRAME NAME: MIPS_70um_fine_FOV4						
Brown Angle	theta_Y(arcmin)	theta_Z(arcmin)	angle(deg)			
WAS(FTB)	+6.296100	-6.809500	-7.187500			
IS (EST)	+6.343290	-6.703954	-8.332868			

dT_EST	+0.047190	+0.105546	-1.145368
T_sSIGMA	+0.002203	+0.002867	+0.186947
dT_EST/T_sSIGMA	+21.417266	+36.817482	-6.126695
<hr/>			
OFFSET	NF	Delta_CW	Delta_CV
5	117	-8.500	+0.000 pixels
OFFSET FRAME NAME: MIPS_SED_8			
Brown Angle	theta_Y(arcmin)	theta_Z(arcmin)	angle(deg)
WAS(FTB)	+5.396307	-8.948538	+0.000049
IS (EST)	+6.385306	-6.709675	-8.332868
dT_EST	+0.988999	+2.238863	-8.332917
T_sSIGMA	+0.002024	+0.002705	+0.186947
dT_EST/T_sSIGMA	+488.699667	+827.674572	-44.573647
<hr/>			
<hr/>			
VARNAME	MEAN	SIGMA	SCALED_SIGMA
a00	-2.7684388276855839E-003	+9.1739671909478009E-003	+5.9139936411323774E-003
b00	-1.2238186984737795E-002	+3.9565995400532294E-003	+2.5506200352962685E-003
c00	-1.0074875370360274E-002	+5.0372929808431008E-003	+3.2472885543586814E-003
del_alpha	+1.4105741314579534E-014	+5.1398578005430046E-003	+3.3134069172091217E-003
beta	+1.0506424023871437E+000	+6.0988321549520583E-003	+3.9316092844009576E-003
del_theta1	+7.0452487160171939E-014	+5.0614223208150979E-003	+3.2628435220393944E-003
del_theta2	-2.0373392312732067E-017	+1.4661680123669680E-006	+9.4516452059320238E-007
del_theta3	+3.5786017055861117E-017	+1.6034034847991965E-006	+1.0336333034446207E-006
del_arx	+6.2098150591184177E-016	+1.5984271649640412E-005	+1.030425321199940E-005
del_ary	-2.6580456367656481E-018	+1.5317952357446236E-006	+9.8747107932207992E-007
del_arz	-1.8836060600690014E-018	+1.5315884299388665E-006	+9.8733776205652402E-007
bgx	+4.4697893987545330E-007	+4.7053556680042622E-007	+3.0333053215299789E-007
bgy	+3.7592617928011074E-009	+1.2478522425374771E-009	+8.0442736210363311E-010
bgz	+2.5961106125531344E-009	+2.5695167503824952E-009	+1.6564377663721766E-009
cgx	-1.1079276663432257E-010	+1.0545010683304428E-010	+6.7978361845757136E-011
cgy	-2.1823607981916954E-013	+2.6285321303890728E-013	+1.6944820033771112E-013
cgz	+4.8965734886587645E-013	+5.7435755444909148E-013	+3.7025932773118392E-013
<hr/>			
LSQF RESIDUAL SIGMA SCALE =	+6.4464953035453121E-001		
<hr/>			
<hr/>			
a_mirror_ipf	a_mirror(1)	a_mirror(2)	a_mirror(3)
a_mirror_ipf	+0.0000000000000000E+000	-7.1354122720146032E-002	+9.9745104600217782E-001
a_mirror_tpf	-2.2059534973642787E-003	+7.3949377026935451E-002	+9.9725955668847632E-001
beta	beta_0	beta	beta_total
	+2.8047410000000001E-006	+1.0506424023871437E+000	+2.9467798223137200E-006
<hr/>			
qT	qT(1)	qT(2)	qT(3)
FrmTbl:	-6.268058023390001E-002	-1.0871044794426700E-003	+9.2407655176308305E-004
Estim:	-7.2652829108634145E-002	-1.1017907337911321E-003	+9.1238959222790723E-004
DelTheta	deltheta(1)	deltheta(2)	deltheta(3)
	-1.9990433238872896E-002	-1.0911740622048235E-005	-2.1283040100331486E-006
[rad]			
EulAngT	theta(1)	theta(2)	theta(3)
[rad]			
Mean	-1.4543598751634887E-001	-2.0651818806358612E-003	+1.9800568965679674E-003
SigmaT	+5.0614223208150979E-003	+1.4661680123669680E-006	+1.6034034847991965E-006
<hr/>			
qR	qR(1)	qR(2)	qR(3)
ASFILE:	+7.0953840622678399E-004	+1.2708605499938130E-003	-1.616350928086501E-004
Estim:	+6.9473479255929046E-004	+1.2703187458470650E-003	-1.6151000473313282E-004
DelThetaR	delthetaR(1)	delthetaR(2)	delthetaR(3)
	-2.9607355035837846E-005	-1.0882416602189378E-006	+2.1333796609585997E-007
[rad]			
EulAngR	angR(1)	angR(2)	angR(3)
[rad]			
Mean	+1.3890627027780065E-003	+2.5408619426997253E-003	-3.2125563994334815E-004
SigmaR	+1.5984271649640412E-005	+1.5317952357446236E-006	+1.5315884299388665E-006
<hr/>			
Initial Gyro Bias	Bg0(1)	Bg0(2)	Bg0(3)
	-3.9629648540540074E-007	-1.8477462049304449E-007	+3.4961990991178027E-007
Gyro Bias Correction	Bg(1)	Bg(2)	Bg(3)
	+4.4697893987545330E-007	+3.7592617928011074E-009	+2.5961106125531344E-009
Total Gyro Bias	BgT(1)	BgT(2)	BgT(3)

+5.0682454470052552E-008 -1.8101535870024339E-007 +3.5221602052433338E-007
 Initial Gyro Bias Rate Cg0(1) Cg0(2) Cg0(3)
 +0.0000000000000000E+000 +0.0000000000000000E+000 +0.0000000000000000E+000
 Gyro Bias Rate Correction Cg(1) Cg(2) Cg(3)
 -1.1079276663432257E-010 -2.1823607981916954E-013 +4.8965734886587645E-013
 Total Gyro Bias Rate CgT(1) CgT(2) CgT(3)
 -1.1079276663432257E-010 -2.1823607981916954E-013 +4.8965734886587645E-013

OFFSET NF Delta_CW Delta_CV
 1 119 -7.500 +0.000 pixels
 OFFSET FRAME NAME: MIPS_70um_fine_FOV1
 qT qT(1) qT(2) qT(3) qT(4)
 WAS(FTB) -6.2680669742346082E-002 -9.9451694379489876E-004 +9.2989163505042877E-004 +9.9803270481394879E-001
 IS (EST) -7.2652938795497043E-002 -1.0094623121563815E-003 +9.066009016997331E-004 +9.9735636035723263E-001

DelTheta deltheta(1) deltheta(2) deltheta(3)
 Units rad rad rad
 -1.9990495603896263E-002 -9.9832724313288396E-006 -2.7171940143879631E-005
 EulAngT theta(1) theta(2) theta(3) [rad]
 Mean -1.4543598751634884E-001 -1.8818539864409213E-003 +1.9550938627219132E-003
 sSigmaT +3.2628436082558225E-003 +5.0017101732182445E-007 +7.077244507272192E-007
 SigmaT +5.0614224545566496E-003 +7.7588052696905020E-007 +1.0978406277338062E-006

OFFSET NF Delta_CW Delta_CV
 2 120 -5.600 -55.000 pixels
 OFFSET FRAME NAME: MIPS_70um_fine_FOV2
 qT qT(1) qT(2) qT(3) qT(4)
 WAS(FTB) -6.2681299506303439E-002 -1.0584007993340006E-003 +2.4477410329351416E-004 +9.9803300274369056E-001
 IS (EST) -7.2653560431802169E-002 -1.0901436671874093E-003 +2.1869533331335850E-004 +9.9735661822425314E-001

DelTheta deltheta(1) deltheta(2) deltheta(3)
 Units rad rad rad
 -1.9990486993598840E-002 -5.6984365733190107E-005 -3.4026030496355105E-005
 EulAngT theta(1) theta(2) theta(3) [rad]
 Mean -1.4543598751634884E-001 -2.1427476530291177E-003 +5.9464151386868710E-004
 sSigmaT +3.2628403640876879E-003 +3.1650383094943946E-006 +3.6687510281978687E-006
 SigmaT +5.0614174221041584E-003 +4.9097038940736551E-006 +5.6910784161747608E-006

OFFSET NF Delta_CW Delta_CV
 3 124 -5.600 +2.500 pixels
 OFFSET FRAME NAME: MIPS_70um_fine_FOV3
 qT qT(1) qT(2) qT(3) qT(4)
 WAS(FTB) -6.2680629031183641E-002 -1.0210205799645107E-003 +9.5003786806900766E-004 +9.9803266163451765E-001
 IS (EST) -7.2652884422976655E-002 -1.0302479652750021E-003 +9.3940246602962558E-004 +9.9735631270732850E-001

DelTheta deltheta(1) deltheta(2) deltheta(3)
 Units rad rad rad
 -1.9990433239141112E-002 +4.7432284167333048E-007 -7.4162161382046530E-007
 EulAngT theta(1) theta(2) theta(3) [rad]
 Mean -1.4543598751634887E-001 -1.9185492030352829E-003 +2.0235440371670151E-003
 sSigmaT +3.2628435955379584E-003 +4.4467223051104093E-007 +6.4732008417106459E-007
 SigmaT +5.0614224348283108E-003 +6.8978911729989028E-007 +1.0041426444770148E-006

OFFSET NF Delta_CW Delta_CV
 4 127 -9.000 +0.000 pixels
 OFFSET FRAME NAME: MIPS_70um_fine_FOV4
 qT qT(1) qT(2) qT(3) qT(4)
 WAS(FTB) -6.2680689147550012E-002 -9.7600930423813318E-004 +9.3105402720938520E-004 +9.9803272078235217E-001
 IS (EST) -7.2652960384396531E-002 -9.9099662704088434E-004 +9.0544316167856845E-004 +9.9735637835517432E-001

DelTheta deltheta(1) deltheta(2) deltheta(3)
 Units rad rad rad
 -1.9990503812152279E-002 -9.7779623007424577E-006 -3.2178189155222108E-005

```

EulAngT      theta(1)          theta(2)          theta(3)          [rad]
Mean        -1.4543598751634884E-001 -1.8451884085620835E-003 +1.9501012582237153E-003
sSigmaT     +3.2628436120957643E-003 +6.4093885056980825E-007 +8.3389729221027486E-007
SigmaT      +5.0614224605132841E-003 +9.9424388041874120E-007 +1.2935668963439174E-006
-----
OFFSET      NF       Delta_CW      Delta_CV
5           117      -8.500      +0.000      pixels
OFFSET FRAME NAME: MIPS_SED_8
qT          qT(1)          qT(2)          qT(3)          qT(4)
WAS(FTB)   +1.4479114620504504E-006 -7.8485974259604125E-004 +1.3015116854428704E-003 +9.9999884502954328E-001
IS (EST)   -7.2652953201003137E-002 -9.9715185542991564E-004 +9.0582907451230868E-004 +9.9735637239305686E-001
DelTheta    deltheta(1)      deltheta(2)      deltheta(3)
Units       rad            rad            rad
-1.4543786262341910E-001 -2.8768907028789355E-004 -6.5125743673394591E-004
EulAngT    theta(1)          theta(2)          theta(3)          [rad]
Mean        -1.4543598751634884E-001 -1.8574102677982025E-003 +1.9517654596389509E-003
sSigmaT     +3.2628436113122041E-003 +5.8868094491166324E-007 +7.8685367475075624E-007
SigmaT      +5.0614224592978015E-003 +9.1317982437358248E-007 +1.2205914030807073E-006
-----
q(1)          q(2)          q(3)          q(4)
PCRS1A: +5.3371888965461637E-007 +3.7444233778550031E-004 -1.4253684912431913E-003 +9.9999891405806784E-001
PCRS2A: -5.2779261998836216E-007 +3.8462959425181312E-004 +1.3722087221825403E-003 +9.9999898455099423E-001
*****
CS-FILE PARAMETERS: ***** AS-FILE PARAMETERS: *****
Row (01) PIX2RADX: +2.473650833999999E-005 Row (1) TASTART: +7.5136200039074707E+008
Row (02) PIX2RADY: +2.546480805700000E-005 Row (2) TASTOP: +7.5137100029077756E+008
Row (03) CXO:      +1.650000000000000000E+001 Row (3) S/C TIME: +7.5135705049076843E+008
Row (04) CYO:      +1.650000000000000000E+001 Row (4) QR1:      +7.0953840622678399E-004
Row (05) BETA0:    +2.8047410000000001E-006 Row (5) QR2:      +1.2708605499938130E-003
Row (06) GAMMA_E0: +8.750000000000000000E+002 Row (6) QR3:      -1.6163509280886501E-004
Row (07) D11:      +1.000000000000000000E+000 Row (7) QR4:      +9.9999892711639404E-001
Row (08) D12:      +0.000000000000000000E+000
Row (09) D21:      +0.000000000000000000E+000
Row (10) D22:      +1.000000000000000000E+000
Row (11) DG:      -1.000000000000000000E+000
-----
INITIAL STA-TO-PCRS ALIGNMENT (R) KNOWLEDGE (1-SIGMA)
SIGMA(X)      SIGMA(Y)      SIGMA(Z)
5.94062910E+000 3.68344177E-001 3.68539668E-001 [arcsec]
-----
PIX2RADX = 2.473650834000E-005[rad/pixel]
XPIXSIZE = 5.1023[arcsec]
PIX2RADY = 2.546480805700E-005[rad/pixel]
YPIXSIZE = 5.2525[arcsec]
CXO = 16.5[pixel] = 84.19[arcsec]
CYO = 16.5[pixel] = 86.67[arcsec]
-----
NOMINAL BETA0 = 2.804741000000E-006[rad/encoder unit]
ENCODER UNIT SIZE = 0.58[arcsec]
GAMMA_E0 = 875.00[encoder unit] = 506.20[arcsec]
-----
| +1 | +0 |
FLIP MATRIX D = |----|----| and DG = -1
| +0 | +1 |

```

3.3 IPF EXECUTION LOG

```
*****
IPF EXECUTION-LOG FILE NAME: LG203118.dat
INSTRUMENT TYPE: MIPS_70um_fine_center
IPF FILTER EXECUTION DATE: 20-Nov-2003 TIME: 15:48
IPF FILTER VERSION USED: IPF.V3.0.0B
*****


----- Loading & Preparing Input Files -----
AAFILE: AA101118 Loaded! AAFILE dimension = 90000 X 21
ASFILE: AS101118 Loaded!
CAFFILE: CA203118 Loaded! CAFFILE dimension = 180 X 15
CBFILE: CB103118 Loaded! CBFILE dimension = 82 X 15
CCFILE: CC203118 Created! CCFILE dimension = 262 X 19
CSFILE: CS203118 Loaded!
Loading Input Files Completed!
-----


----- Selected Mask Vectors -----
index = 1 2 3 4 5 6 7 8 9 10 11 12 13 14 15 16 17 18 19 20
-----
mask1 = [ 1 1 1 0 0 0 0 0 0 0 0 0 0 0 0 0 0 0 0 0 ]
mask2 = [ 1 1 1 1 1 1 1 0 0 0 0 0 0 1 1 1 1 1 1 ]


----- Selected Initial Gyro Bias Parameters -----
User Entered 1 : Use AFILE database - from S/C filter
IPF Linearized Using Following Nominal Gyro Bias Estimates
bg0 = [-3.9629648540540074E-007 -1.8477462049304449E-007 +3.4961990991178027E-007 ]
cg0 = [+0.0000000000000000E+000 +0.0000000000000000E+000 +0.0000000000000000E+000 ]


----- Gyro Pre-Processor Run Completed -----
AGFILE CREATED: AG203118.m ACFILE CREATED: AC203118.m
-----


Total Gyro Preprocessor Execution Time: 57 seconds

FRAME TABLE ENTRIES FOR PCRS LOADED TO TPCRS
q_PCRS4 = [ +5.3371888965461637E-007 q_PCRS5 = [ +7.3379987833742897E-007
            +3.7444233778550031E-004 +5.2236196154513707E-004
            -1.4253684912431913E-003 -1.4047712280184723E-003
            +9.9999891405806784E-001 ]; +9.9999887687698918E-001 ];
q_PCRS8 = [ -5.2779261998836216E-007 q_PCRS9 = [ -7.1963421681856818E-007
            +3.8462959425181312E-004 +5.3239763239987400E-004
            +1.3722087221825403E-003 +1.3516841804518383E-003
            +9.9999898455099423E-001 ]; +9.9999894475050310E-001 ];

----- Initial Conditions for State ----- ----- Initial Square-Root Cov (diag) -----
p1(01) = a00 = +0.0000000000000000E+000 Sigma_initial(01,01) = 1.0000000000000000E+000
p1(02) = b00 = +0.0000000000000000E+000 Sigma_initial(02,02) = 1.0000000000000000E+000
p1(03) = c00 = +0.0000000000000000E+000 Sigma_initial(03,03) = 1.0000000000000000E+000
p1(04) = a10 = +0.0000000000000000E+000 Sigma_initial(04,04) = 9.9999000000000000E+004
p1(05) = b10 = +0.0000000000000000E+000 Sigma_initial(05,05) = 9.9999000000000000E+004
p1(06) = c10 = +0.0000000000000000E+000 Sigma_initial(06,06) = 9.9999000000000000E+004
p1(07) = d10 = +0.0000000000000000E+000 Sigma_initial(07,07) = 9.9999000000000000E+004
p1(08) = a20 = +0.0000000000000000E+000 Sigma_initial(08,08) = 9.9999000000000000E+004
p1(09) = b20 = +0.0000000000000000E+000 Sigma_initial(09,09) = 9.9999000000000000E+004
p1(10) = c20 = +0.0000000000000000E+000 Sigma_initial(10,10) = 9.9999000000000000E+004
p1(11) = d20 = +0.0000000000000000E+000 Sigma_initial(11,11) = 9.9999000000000000E+004
p1(12) = a01 = +0.0000000000000000E+000 Sigma_initial(12,12) = 9.9999000000000000E+004
p1(13) = b01 = +0.0000000000000000E+000 Sigma_initial(13,13) = 9.9999000000000000E+004
p1(14) = c01 = +0.0000000000000000E+000 Sigma_initial(14,14) = 9.9999000000000000E+004
p1(15) = d01 = +0.0000000000000000E+000 Sigma_initial(15,15) = 9.9999000000000000E+004
p1(16) = e01 = +0.0000000000000000E+000 Sigma_initial(16,16) = 9.9999000000000000E+004
p1(17) = f01 = +0.0000000000000000E+000 Sigma_initial(17,17) = 9.9999000000000000E+004
```

```

-----
p2f(01) = am1 = +0.000000000000000E+000 Sigma_initial(18,18) = 1.0000000000000001E-001
p2f(02) = am2 = +0.000000000000000E+000
p2f(03) = am3 = +1.000000000000000E+000
p2f(04) = beta = +1.000000000000000E+000 Sigma_initial(19,19) = 1.0000000000000001E-001
p2f(05) = qT1 = -6.2680580233390057E-002 Sigma_initial(20,20) = 1.0000000000000001E-001
p2f(06) = qT2 = -1.0871044794426709E-003 Sigma_initial(21,21) = 1.0000000000000000E-002
p2f(07) = aT3 = +9.2407655176308381E-004 Sigma_initial(22,22) = 1.0000000000000000E-002
p2f(08) = qT4 = +9.9803261928054376E-001
p2f(09) = QR1 = +7.0953840622678399E-004 Sigma_initial(23,23) = 2.8800982630534152E-004
p2f(10) = QR2 = +1.2708605499938130E-003 Sigma_initial(24,24) = 1.7857829658811045E-005
p2f(11) = QR3 = -1.6163509280886501E-004 Sigma_initial(25,25) = 1.7867307310572328E-005
p2f(12) = QR4 = +9.9999892711639404E-001
p2f(13) = brx = +0.000000000000000E+000 Sigma_initial(26,26) = 9.999900000000000E+004
p2f(14) = bry = +0.000000000000000E+000 Sigma_initial(27,27) = 9.999900000000000E+004
p2f(15) = brz = +0.000000000000000E+000 Sigma_initial(28,28) = 9.999900000000000E+004
p2f(16) = crx = +0.000000000000000E+000 Sigma_initial(29,29) = 9.999900000000000E+004
p2f(17) = cry = +0.000000000000000E+000 Sigma_initial(30,30) = 9.999900000000000E+004
p2f(18) = crz = +0.000000000000000E+000 Sigma_initial(31,31) = 9.999900000000000E+004
p2f(19) = bgx = +0.000000000000000E+000 Sigma_initial(32,32) = 1.3676930256637773E-004
p2f(20) = bgy = +0.000000000000000E+000 Sigma_initial(33,33) = 1.3676930256637773E-004
p2f(21) = bgz = +0.000000000000000E+000 Sigma_initial(34,34) = 1.3676930256637773E-004
p2f(22) = cgx = +0.000000000000000E+000 Sigma_initial(35,35) = 1.8705842124493380E-008
p2f(23) = cgy = +0.000000000000000E+000 Sigma_initial(36,36) = 1.8705842124493380E-008
p2f(24) = cgz = +0.000000000000000E+000 Sigma_initial(37,37) = 1.8705842124493380E-008
-----
```

```

----- IPF KALMAN FILTER STARTED -----
Iteration#001: |dp|= +1.606095146421E-001 RMS(|Res|)=+2.754191397497E-005
Iteration#002: |dp|= +7.422825368706E-002 RMS(|Res|)=+2.100103874777E-005
Iteration#003: |dp|= +2.084412258979E-003 RMS(|Res|)=+1.457901475006E-005
Iteration#004: |dp|= +1.428296028465E-003 RMS(|Res|)=+1.458135071283E-005
Iteration#005: |dp|= +8.929238055280E-005 RMS(|Res|)=+1.455494477936E-005
Iteration#006: |dp|= +2.615546832676E-005 RMS(|Res|)=+1.455615402791E-005
Iteration#007: |dp|= +2.545000368493E-006 RMS(|Res|)=+1.455658472083E-005
Iteration#008: |dp|= +3.946207277013E-007 RMS(|Res|)=+1.455654177533E-005
Iteration#009: |dp|= +6.902358507789E-008 RMS(|Res|)=+1.455653552008E-005
Iteration#010: |dp|= +4.997145244056E-009 RMS(|Res|)=+1.455653670848E-005
Iteration#011: |dp|= +1.557944909133E-009 RMS(|Res|)=+1.455653678058E-005
Iteration#012: |dp|= +5.212136415206E-011 RMS(|Res|)=+1.455653675411E-005
Iteration#013: |dp|= +3.161158895602E-011 RMS(|Res|)=+1.455653675403E-005
Iteration#014: |dp|= +1.676837172115E-012 RMS(|Res|)=+1.455653675457E-005
Iteration#015: |dp|= +5.779697226526E-013 RMS(|Res|)=+1.455653675455E-005
Iteration#016: |dp|= +2.709622176286E-013 RMS(|Res|)=+1.455653675453E-005
Iteration#017: |dp|= +4.882912833384E-013 RMS(|Res|)=+1.455653675454E-005
Iteration#018: |dp|= +4.950483834122E-013 RMS(|Res|)=+1.455653675454E-005
Iteration#019: |dp|= +1.697552733252E-013 RMS(|Res|)=+1.455653675454E-005
Iteration#020: |dp|= +2.600220721133E-013 RMS(|Res|)=+1.455653675454E-005
Iteration#021: |dp|= +8.951647956080E-013 RMS(|Res|)=+1.455653675454E-005
Iteration#022: |dp|= +7.917467230399E-013 RMS(|Res|)=+1.455653675455E-005
Iteration#023: |dp|= +1.004663247129E-013 RMS(|Res|)=+1.455653675454E-005
Iteration#024: |dp|= +6.309141570211E-013 RMS(|Res|)=+1.455653675454E-005
Iteration#025: |dp|= +2.999059379956E-013 RMS(|Res|)=+1.455653675454E-005
Iteration#026: |dp|= +1.478056212685E-013 RMS(|Res|)=+1.455653675454E-005
Iteration#027: |dp|= +4.208453826432E-013 RMS(|Res|)=+1.455653675454E-005
Iteration#028: |dp|= +4.129739279150E-013 RMS(|Res|)=+1.455653675454E-005
Iteration#029: |dp|= +1.144363712982E-013 RMS(|Res|)=+1.455653675454E-005
Iteration#030: |dp|= +2.374176355860E-013 RMS(|Res|)=+1.455653675454E-005
IPF Kalman Filter Completed with Error |dp1| + |dp2| = +2.3741763558595759E-013
-----
```

```

----- IPF LEAST SQUARES FILTER STARTED -----
Iteration#001 COND#=+1.152907823242E+008, |dp|=+1.613933753154E-001
Iteration#002 COND#=+1.069844409449E+008, |dp|=+7.574018030773E-002
Iteration#003 COND#=+1.088098487918E+008, |dp|=+2.652049493974E-003
Iteration#004 COND#=+1.087644528582E+008, |dp|=+3.608052415528E-004
Iteration#005 COND#=+1.087566842894E+008, |dp|=+2.234591578391E-005
Iteration#006 COND#=+1.087562063054E+008, |dp|=+1.430393274470E-006
-----
```

```

Iteration#007 COND#=+1.087561757159E+008, |dp|=+9.201484688695E-008
Iteration#008 COND#=+1.087561737279E+008, |dp|=+5.920344739901E-009
Iteration#009 COND#=+1.087561736549E+008, |dp|=+3.815554086090E-010
Iteration#010 COND#=+1.087561736094E+008, |dp|=+2.463064805495E-011
Iteration#011 COND#=+1.087561735541E+008, |dp|=+1.946618318670E-012
Iteration#012 COND#=+1.087561736132E+008, |dp|=+5.881102640320E-013
Iteration#013 COND#=+1.087561735892E+008, |dp|=+3.942028319437E-013
Iteration#014 COND#=+1.087561736231E+008, |dp|=+6.436922834642E-013
Iteration#015 COND#=+1.087561736237E+008, |dp|=+6.087119373896E-013
Iteration#016 COND#=+1.087561736144E+008, |dp|=+1.294869783040E-013
Iteration#017 COND#=+1.087561735580E+008, |dp|=+4.569596937712E-013
Iteration#018 COND#=+1.087561736444E+008, |dp|=+5.459282824613E-013
Iteration#019 COND#=+1.087561736080E+008, |dp|=+1.258778336120E-012
Iteration#020 COND#=+1.087561736136E+008, |dp|=+8.156144266215E-013
Iteration#021 COND#=+1.087561736108E+008, |dp|=+5.651948414117E-013
Iteration#022 COND#=+1.087561736137E+008, |dp|=+1.546521513708E-013
Iteration#023 COND#=+1.087561735612E+008, |dp|=+1.485967902714E-013
Iteration#024 COND#=+1.087561735506E+008, |dp|=+3.253329182980E-013
Iteration#025 COND#=+1.087561736471E+008, |dp|=+6.004975514871E-013
Iteration#026 COND#=+1.087561736464E+008, |dp|=+1.550890619895E-012
Iteration#027 COND#=+1.087561736290E+008, |dp|=+1.144966786855E-012
Iteration#028 COND#=+1.087561735926E+008, |dp|=+2.881281568393E-013
Iteration#029 COND#=+1.087561735675E+008, |dp|=+3.154518501611E-013
Iteration#030 COND#=+1.087561735987E+008, |dp|=+2.467304523341E-013
IPF Least Squares Filter Completed with Error |dp1| + |dp2| = +2.4673045233408786E-013
-----
```

Total Execution Time: 405 seconds

4 COMMENTS

This run is actually a re-run of the Coarse Survey IC202118 using FF003118.m (provided by the MIPS science team). Overall the data looked clean, and the filter converged nicely.

1. The run was performed in normal IPF operating mode.
2. This run uses IPF version 3.0 where the gyro drift bias estimates make use of the recently corrected GCF signs, (MCR 2521) and now show no sandwich-to-sandwich variations.
3. There were 10 sandwich maneuvers with 180 science centroids and 82 PCRS measurements. No science centroids were removed. However, 3 PCRS centroids were removed from the original 85 centroids, at the 3-sigma level.
4. We estimated 17 parameters consisting of: 3 constant plate scales, 2 mirror parameters, 3 IPF alignment angles, 3 STA-to-PCRS alignment angles, and 3 gyro bias and 3 gyro bias-drift parameters.
5. The scan mirror parameter estimates (alpha and beta) indicate that the mirror spin axis is tilted by 4 degrees with a 0.2 degree confidence and the scan mirror scale factors are off by 5 percent with a 1-sigma confidence of about 0.4 percent. These values are consistent with those obtained earlier from the Coarse Focal Plane Survey results when considering their reported uncertainties.
6. Constant plate scales were estimated at about the 1 percent level. This is significantly smaller than previous reported level of about 7 percent in the W direction and 4 percent in the V direction. This is understandable given the fact that the previous data set (Run IC102118) contained a large number of bad centroids (about half the total), and the retained centroids did not provide an adequate spatial sampling of the array (i.e., the centroids were isolated in a smaller section of the instrument FOV). The current estimates of plate scales are expected to be more accurate.

We recommend updating frames 118, 119, 120, 124, 127 and 117 with the new quaternions listed in the IF file IF203118.dat. This contains adjustments of 2.3 and 0.15 arcseconds in Y and Z, and 1.15 deg in twist (for the prime frame). In our best judgement, this coarse survey is accurate to 0.3 arcsecond which satisfies its coarse survey requirement of 1.12 arcseconds by a good margin.

IPF TEAM CONTACT INFORMATION

IPF Team email	ipf@sirtfweb.jpl.nasa.gov	
David S. Bayard	X4-8208	David.S.Bayard@jpl.nasa.gov (TEAM LEADER)
Dhemetrio Boussalis	X4-3977	boussali@grover.jpl.nasa.gov
Paul Brugarolas	X4-9243	Paul.Brugarolas@jpl.nasa.gov
Bryan H. Kang	X4-0541	Bryan.H.Kang@jpl.nasa.gov
Edward.C.Wong	X4-3053	Edward.C.Wong@jpl.nasa.gov (TASK MANAGER)

ACKNOWLEDGEMENTS

This work was performed at the Jet Propulsion Laboratory, California Institute of Technology, under contract with the National Aeronautics and Space Administration.

References

- [1] D.S. Bayard, B.H. Kang, *SIRTF Instrument Pointing Frame Kalman Filter Algorithm*, JPL D-Document D-24809, September 30, 2003.
- [2] B.H. Kang, D.S. Bayard, *SIRTF Instrument Pointing Frame (IPF) Software Description Document and User's Guide*, JPL D-Document D-24808, September 30, 2003.
- [3] D.S. Bayard, B.H. Kang, *SIRTF Instrument Pointing Frame (IPF) Kalman Filter Unit Test Report*, JPL D-Document D-24810, September 30, 2003.
- [4] *Space Infrared Telescope Facility In-Orbit Checkout and Science Verification Mission Plan*, JPL D-Document D-22622, 674-FE-301 Version 1.4, February 8, 2002.
- [5] *Space Infrared Telescope Facility Observatory Description Document*, Lockheed Martin LMMS/P458569, 674-SEIT-300 Version 1.2, November 1, 2002.
- [6] *SIRTF Software Interface Specification for Science Centroid INPUT Files (CAFILER, CSFILE)*, JPL SOS-SIS-2002, November 18, 2002.
- [7] *SIRTF Software Interface Specification for Inferred Frames Offset INPUT Files (OFILE)*, JPL SOS-SIS-2003, November 18, 2002.
- [8] *SIRTF Software Interface Specification for PCRS Centroid INPUT Files (CBFILE)*, JPL SIS-FES-015, November 18, 2002.
- [9] *SIRTF Software Interface Specification for Attitude INPUT Files (AFILE, ASFILE)*, JPL SIS-FES-014, January 7, 2002.
- [10] *SIRTF Software Interface Specification for IPF Filter Output Files (IFFILE, LGFILE, TARFILE)*, JPL SOS-SIS-2005, November 18, 2002.
- [11] R.J. Brown, *Focal Surface to Object Space Field of View Conversion*. Systems Engineering Report SER No. S20447-OPT-051, Ball Aerospace & Technologies Corp., November 23, 1999.